Drift og vedlikehold
Fagressurser Drift og vedlikehold
Geofag Drift og vedlikehold
8.11.2022

Statens vegvesen

Field test of UAS to support avalanche monitoring

Geohazard Survey from Air (GEOSFAIR) - Report from field test at Fonnbu March 2022

STATENS VEGVESENS RAPPORTER Nr. 873

Photo: Richard Moore, SINTEF

Tittel
Field test of UAS to support avalanche monitoring

Undertittel
Geohazard Survey from Air (GEOSFAIR) - Report from field test at Fonnbu March 2022

Forfatter
Regula Frauenfelder (editor) with co-authors from NGI, SINTEF and NPRA (see page 3)

Avdeling
Fagressurser Drift og vedlikehold

Seksjon
Geofag Drift og vedlikehold

Prosjektnummer
C15115

Rapportnummer
873

Prosjektleder
Tore Humstad

Godkjent av
Tore Humstad

Emneord
GEOSFAIR, NGI, SINTEF, droner, snøskred, snø, lidar, fotogrammetri

Sammendrag
I mars/april 2022 gjennomførte Statens vegvesen, Norges geotekniske institutt og SINTEF en felttest med UAS med ulike instrumenter på forskningsstasjonen Fonnbu i Stryn.

Formålet med testen var å evaluere bruken av instrumenterte droner til overvåking og vurdering av snøskredfare. Instrumentene som ble testet inkluderte optisk og termisk avbildning, laserskanning og georadar.

Resulterende datasett inkluderte 3D-modeller (punktskyer og høydekart), multispektrale og radiometriske, termiske bilder og radargrammer.

Antall sider 71

Title
Field test of UAS to support avalanche monitoring

Subtitle
Geohazard Survey from Air (GEOSFAIR) - Report from field test at Fonnbu March 2022

Author
Regula Frauenfelder (editor) with co-authors from NGI, SINTEF and NPRA (see page 3)

Department
Planning and Engineering Services

Section
Geomechanics

Project number
C15115

Report number
873

Project manager
Tore Humstad

Approved by
Tore Humstad

Key words
GEOSFAIR, NPRA, NGI, SINTEF, UAS, AVALANCHE, SNOW, LIDAR, SFM, PHOTOGRAMMETRY

Summary
In March/April 2022, the Norwegian Public Roads Administration, the Norwegian Geotechnical Institute and SINTEF performed a field test with UAS carrying different instruments at the research station Fonnbu in Stryn, Norway.

The overall purpose was to evaluate the practical performance of UAS and sensors in field conditions towards the goal of assessing and monitoring snow avalanche hazard. The devices tested included optical and thermal imaging, laser scanning, and ground penetrating radar.

Resulting geospatial datasets included 3D models (point clouds and elevation maps), multispectral and radiometric thermal images, and radargrams.

Pages 71

REPORT

GEOSFAIR (Geohazard Survey from Air – remote decision support with focus on avalanche applications)

FIELD TEST ACTIVITY REPORT
FONNBU MARCH 2022

DOC.NO. 20210309-01-R
REV.NO. 0 / 2022-11-08

NORWEGIAN GEOTECHNICAL INSTITUTE
NGI.NO

Project

Project title:	GEOSFAIR (Geohazard Survey from Air – remote decision support with focus on avalanche applications)
Document title:	Field test activity report - Fonnbu March 2022
Document no.:	20210309-01-R
Date:	2022-11-08
Revision no. /rev. date:	0 / 2022-11-08

Client

Client:	The Research Council of Norway
Client contact person:	Mette Brest Jonassen
Contract reference:	321035/O80
Project manager:	Tore Humstad, Norwegian Public Roads Administration
Prepared by (in alphabetical order):	*NGI*: Regula Frauenfelder, Sean Salazar *NPRA*: Halgeir Dahle, Tore Humstad, Edward McCormack, Emil Solbakken *SINTEF Digital*: Trine Kirkhus, Richard Moore *SINTEF Industry*: Bastien Dupuy, Arnt Grøver, Pauline Lorand
Reviewed by:	Regula Frauenfelder, Tore Humstad, Edward McCormack, Sean Salazar

Summary

This report documents a field test that was completed as part of the GEOSFAIR (Geohazard Survey from Air) research project which is funded by the Norwegian Public Roads Administration (NPRA) and the Research Council of Norway (Innovation Project for the Public Sector, grant no. 321035). The main goal of the GEOSFAIR project is to develop effective methodologies for evaluating natural hazards by integrating uncrewed aerial systems (UAS or drones) and UAS-collected data into the NPRA's decision support system. The tests were completed at Norwegian Geotechnical Institute's Fonnbu avalanche research station in April of 2022. The project team included staff from the NPRA, the Norwegian Geotechnical Institute (NGI), and the research organization SINTEF (staff from both the Digital and the Industry groups).

The overall purpose of the test was to evaluate the practical performance of UAS and sensors in field conditions towards the goal of assessing and monitoring snow avalanche hazard. The devices tested included optical and thermal imaging, laser scanning, and ground penetrating radar. Resulting geospatial datasets included 3d models (point clouds and elevation maps), multispectral and radiometric thermal images, and radargrams.

Various measurements and flights were carried out over pre-defined test areas. The UAS-based measurements were complemented by manually dug snow pit characterization. The sensors used during the test provided promising and detailed datasets about the snowpack characteristics and the surround terrain. In most cases, the operation of the UAS flight planning, communications systems, flight controls, and automated flights worked well. The use of each sensor also presented challenges which will be further explored. These challenges included equipment failures, difficulties operating UAS at altitude and speeds suitable for collection of data and images, some manufacture-caused problems with the radar equipment due to low temperatures, and complex and time-consuming data processing.

Contents

Appendix

Review and reference page

1 Introduction

This report documents a four-day field test of uncrewed aerial systems (UAS) used to monitor snow conditions and associated avalanche danger. The test occurred at the Norwegian Geotechnical Institute's avalanche research station 'Fonnbu' at Strynefjellet, Vestland county, Norway, March 29 to April 1, 2022. The test was conducted as part of the GEOSFAIR (Geohazard Survey from Air) research project which is funded by the Norwegian Public Roads Administration (NPRA) and the Research Council of Norway (Innovation Project for the Public Sector, grant no. 321035).

The test described herein is the second field test performed within the GEOSFAIR project. The first test, the Trollstigen field test, was conducted October 25–27, 2021. The first test focussed on portable lidar scanners from UAS and was performed in collaboration with seven vendor companies (see NPRA report 825[1]). A third test is planned in 2023.

GEOSFAIR aims to develop effective methodologies for integrating UAS aerial systems and UAS-collected data into the NPRA decision support system for geohazard risk assessment, considering both decision-making requirements and UAS aircraft, sensors, and software specifications. The project, which has a focus on snow avalanches, aims to foster the uptake of instrumented UAS into the NPRA's operations to support faster and better assessments of avalanche danger to roads. In addition, applications for other geohazards will be evaluated.

The project team included staff from the NPRA, the Norwegian Geotechnical Institute (NGI), and the research organization SINTEF (with staff from both the Digital and the Industry groups).

The GEOSFAIR project is organized across four work packages:

- *WP1: Hardware – aircraft platforms and sensors*. This work package will provide optimal user-guided specifications of the UAS flight system, the associated sensors and logistical aspects required to forecast and monitor avalanches and relevant snow parameters in harsh conditions.
- *WP2: Software – mission planning, automation, and processing workflow*. This package will provide optimized software guidelines and testing environments to prepare for autonomous UAS flight and data recording as well as automated data processing and interpretation workflows.
- *WP3: Application – field demonstrations and interpretation of results*. This package consolidates the requirements for application of UAS into NPRA operations, followed by testing of UAS under varying field conditions, while considering the UAS specifications that were derived in WP1 and WP2. Data gathered by UAS will be interpreted and validated using conventional instrumentation and methods such as hand dug snow pits.

[1] https://hdl.handle.net/11250/2999621

- *WP4: Integration – enhanced decision support*. This work package will investigate and pilot how the outcomes of WP1, WP2 and WP3, i.e. the aerial systems and the sensor data output, can be integrated into the NPRA's decision support processes with an emphasis on snow avalanches.

A website with information on the GEOSFAIR effort can be found on NPRA's webpage[2].

Fonnbu has been NGI's avalanche research station at Strynefjellet (Figure 1-1) since 1973. Fonnbu is a meeting place for applied avalanche research and is used for training and educational purposes, as well as by other avalanche experts from Norway and abroad. Since NGI is a part of the GEOSFAIR team, Fonnbu was a natural location to perform at least one of the three planned GEOSFAIR field tests. Figure 1-2 depicts the research team at Fonnbu. Fonnbu is also located close to Ryggfonn, NGI's avalanche test facility[3], in operation since 1981. The facility is one of only two in the world capable of experiments at this scale[4], and the catchment dam in the runout zone is a unique feature making this location the only place in the world where the efficiency of avalanche mitigation can be studied at full-scale.

Figure 1-1. Fonnbu avalanche research station during the field test in March 2022. (Photo: Regula Frauenfelder)

[2] https://www.vegvesen.no/fag/fokusomrader/forskning-innovasjon-og-utvikling/pagaende-programmer-og-prosjekter/geosfair/
[3] https://www.ngi.no/eng/Services/Technical-expertise/Avalanches/Ryggfonn
[4] https://www.youtube.com/watch?reload=9&v=j1nE4U-c9s8&feature=emb_imp_woyt

The Fonnbu field test was conducted mainly in the context of the work outlined in work packages 1–3. The test explored the operation of different UAS platforms and sensors and associated aspects including mission and flight planning, communications systems, flight controls, automated flights, and use of Global Navigation Satellite System (GNSS) positioning in a mountain environment with cold and dry winter conditions. The test also evaluated the use of the following sensor and imaging techniques to collect information on snow and terrain conditions related to avalanche hazards:

- Thermal (radiometric infrared) images
- Optical (RGB and multispectral) images
- Photogrammetry (Structure-from-Motion or SfM)
- Lidar (laser scanning)
- Ground penetrating radar (GPR)

The responsibilities for each GEOSFAIR group during the field tests were:

NPRA

- Flight safety and flight coordination
- Avalanche safety for the field work (in cooperation with NGI)
- Installation and measurement of ground control points
- Lidar and photogrammetry testing
- Evaluation of flight planning software
- Snowpack observations

NGI

- Access to Fonnbu research station and all associated logistics, including safety precautions (avalanche safety in cooperation with NPRA)
- Monitoring of the field demonstrations and interpretation of results
- Testing of UAS operations under varying field conditions
- Testing of thermal imaging
- Snowpack observations

SINTEF (Industry)

- Testing of ground penetrating radar
- Exploring automatic terrain-following flight programs
- Data processing of Structure-from-Motion survey data
- Testing a SnowScope probe (a digital snow penetrometer) used to derive snow hardness profiles

SINTEF (Digital)

- Recommendations for sensor technologies
- Testing a multispectral imaging camera

In addition to information about the field test site and snow and weather conditions, this document includes the reports as completed by each of the four GEOFAIR groups noted

above. Each group provided information about the work packages they addressed, their goals and activities during the test, their findings, and next steps. The report concludes with a summary of the findings and how these will guide the next steps for GEOSFAIR.

Figure 1-2. GEOSFAIR's Fonnbu field test participants. (Photo: Regula Frauenfelder)

1.1 Test sites

The research team reviewed maps and used local knowledge to select four survey areas with varied terrain around the research station, as well as to designate a safe access area with low avalanche risk and to provide areas to support simultaneous flight operations. The four survey areas (A1, A2, B and C) are shown in Figure 1-3.

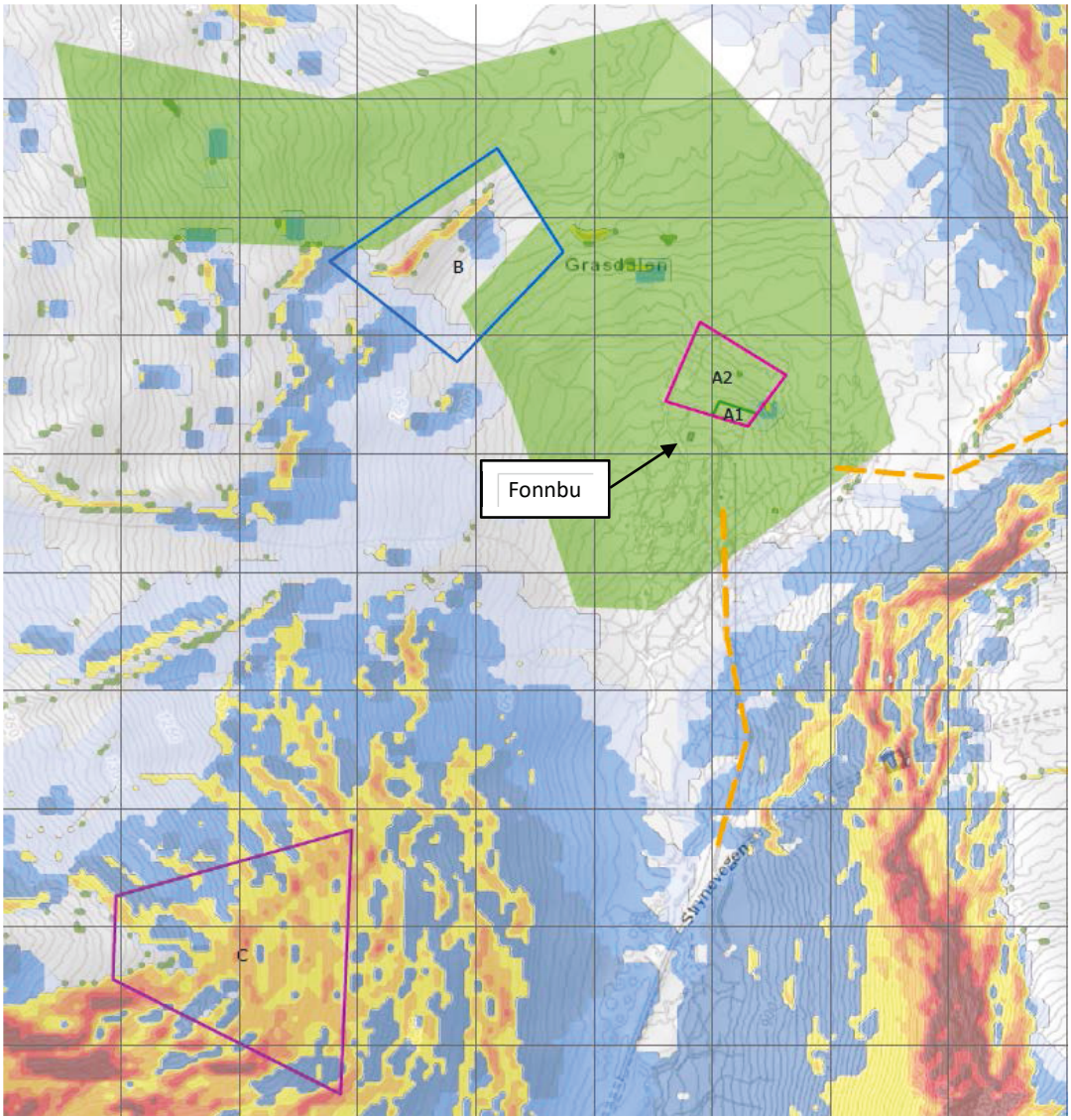

Figure 1-3. Survey area locations. Green = safe access area. See Appendix A for full legend, scale and coordinates. The research station Fonnbu is situated just south of area A1/A2, as indicated by the label on the map.

1.2 Weather

The weather during the test week did not provide any notable difficulties for flying the UAS (Figure 1-4). The weather was largely calm and there was good visibility. Air temperature (as measured at the local weather station at Fonnbu) ranged from -16,5°C to +3,4°C.

There were a few centimetres of new snow (~3-4 cm) on the first day of the field test, but that was the only precipitation for the duration of the Fonnbu test.

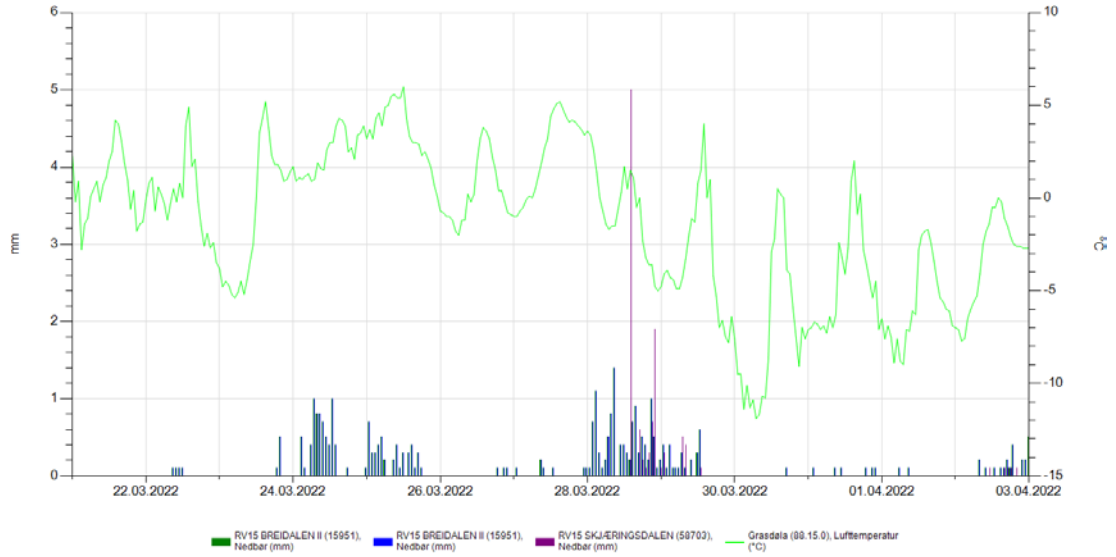

Figure 1-4: Precipitation and temperature in the days prior to and during the Fonnbu field test (29.3. to 1.4.22). Precipitation as measured at stations no. 15951 (RV15 Breidalen II) and 58703 (RV15 Skjæringsdalen), temperature as measured at station no. 88.15.0 (Grasdøla). Source: xgeo/NPRA. Locally at Fonnbu, temperatures were slightly colder, maximum temperatures reaching +3,4°C and minimum temperatures down to -16,5°C (cf. Appendix B).

1.3 Snow observations

The snow observations were used to correlate the field conditions with the data collected by the various technologies used in the test. The snow pack at the Fonnbu station was roughly 2.5 m deep, with varying snow depths (up to 12–15 m in cornice areas) in the terrain around the station, depending on location and topography.

Investigations of snowpack properties were conducted at different locations around test areas A and B (Figure 1-5) and were used to ground-truth measurement obtained by the ground penetrating radar, as well as multispectral and infrared cameras. Based on avalanche safety considerations, no in-situ measurements were carried out in test area C.

In total, 15 sets of observations between March 29 and April 1, 2022 were uploaded to Regobs.no, which is the Varsom-platform run by the Norwegian Water and Energy Directorate. This site facilitates registering and sharing field observations. An overview of the observations and links to the online registrations in the Regobs database are found in Table 1-1. Some examples of observations are shown in Figure 1-7 and Figure 1-8. The locations of the registered snow pits are depicted on the map in Figure 1-5.

Table 1-1: Location information for snow cover investigations around survey areas A2 and B with hyperlinks to more documentation in Varsom Regobs.

			Observation date		
Test site no.	**Location**	**Aspect, Inclination**	**29.3.2022**	**30.3.2022**	**31.1.2022**
A2-1	N 62.0004215, E 7.3129661, 953 m asl	Aspect N213° Inclination 22°	Snow surface, sun exposed new snow (regobs 305382, at 15:39)	Snow surface, wind affected (regobs 305388, at 09:58)	Snow profile (regobs 299587, 12:00–15:00)
A2-2	N 62.0007093 E 7.3122461 958 m asl	Aspect N218° Inclination 20°	Snow surface, sun exposed new snow (regobs 305383, at 15:50)	Snow surface, wind affected (regobs 305389, at 10:07)	
A2-3	N 62.0018806 E 7.3122854 983 m asl	Aspect N220° Inclination 5°	Snow surface, partly sun- exposed new snow (regobs 305385, at 16:11)	Snow surface, new snow still intact (regobs 305390, at 10:26)	
A2-4	N 62.001656 E 7.3134398 983 m asl	Aspect N30° Inclination 20°	Snow surface, shaded new snow (regobs 305386, at 16:20)	Snow surface, shaded, a little wind affected (regobs 305391, at 10:37; Figure 1-6)	
A2-5	N 62.000197 E 7.3171763 982 m asl	Aspect N260° Inclination unknown		Snow pit (regobs 298484, at 16:00)	
B-1	N 62.0027966, E 7.2990792, 1095 m asl	Aspect 90° Inclination 20°	Snow pit (regobs 298284 at 18:09)	Snow pit (regobs 305508, at 14:34)	
B-2	N 62.0008635 E 7.3077697 960 m asl	Aspect N135° Inclination 15°		Snow pit (regobs 298495,at 11:10) Snow surface (regobs 305502, at 14:20)	

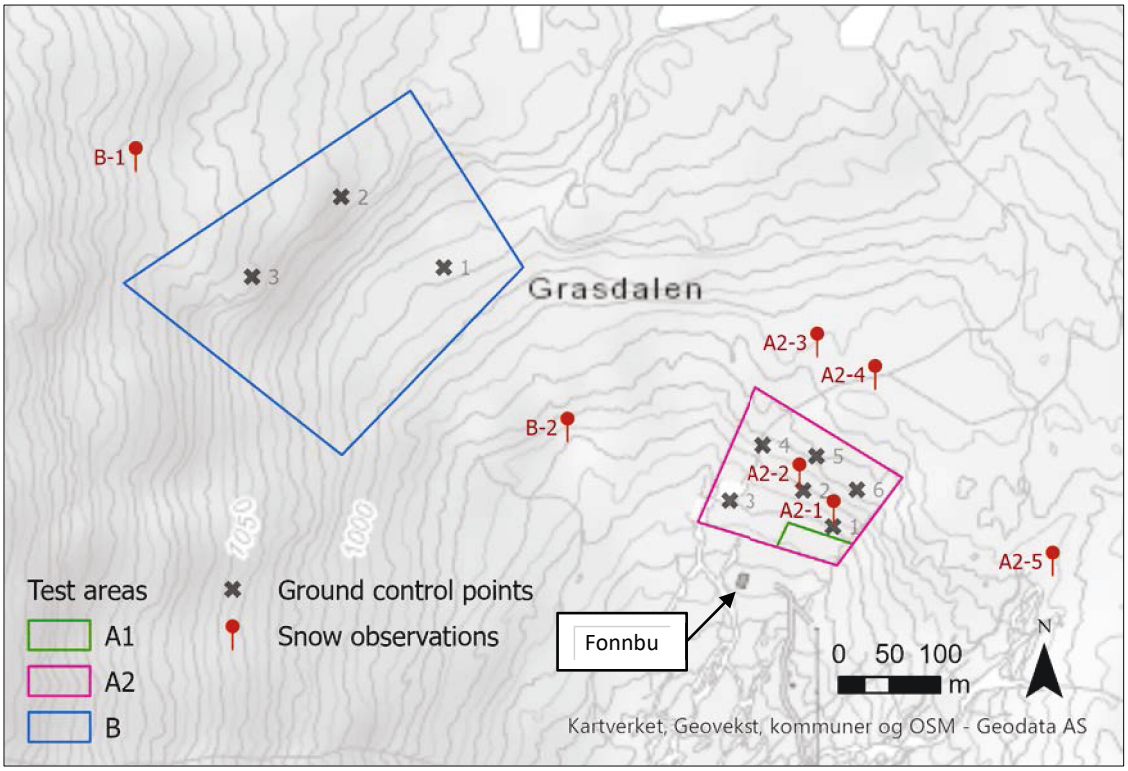

Figure 1-5. Map showing survey areas A1/2 and B, snow observation locations and ground control points (GCPs).

Figure 1-6. Example of a Varsom Regobs registered snow surface observation located close to Fonnbu. https://www.regobs.no/registration/305391

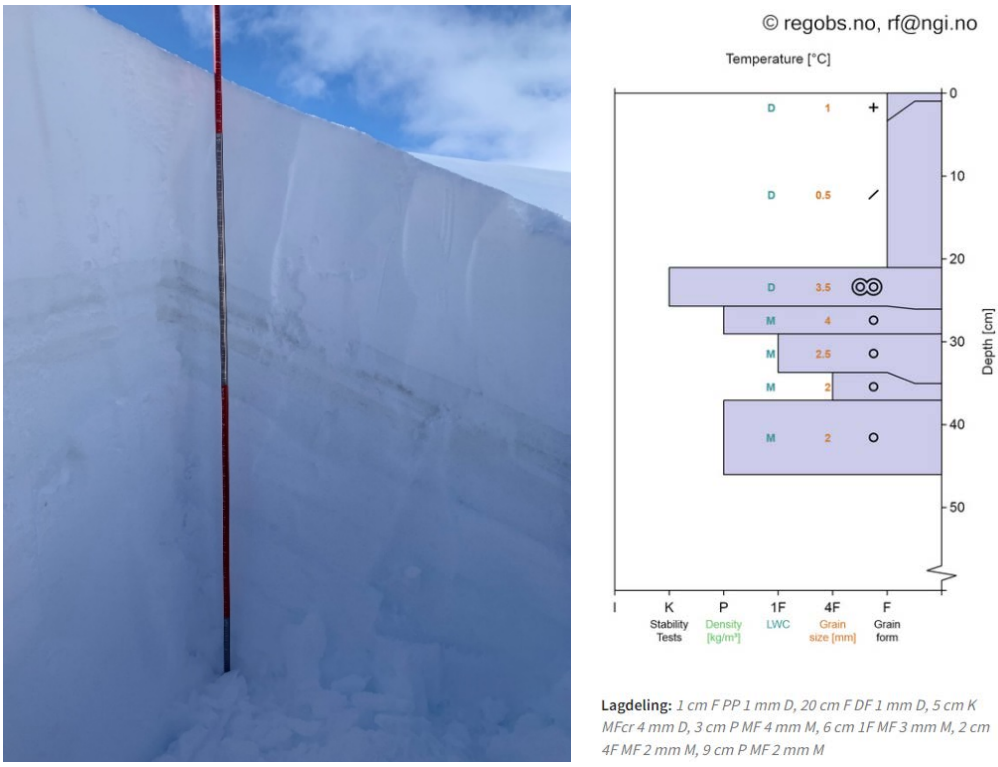

Figure 1-7. Example of a Varsom Regobs registered snow pit observation located close to Fonnbu; snow pit (left) and snow profile information (right), [https://regobs.no/registration/298495.](https://regobs.no/registration/298495)

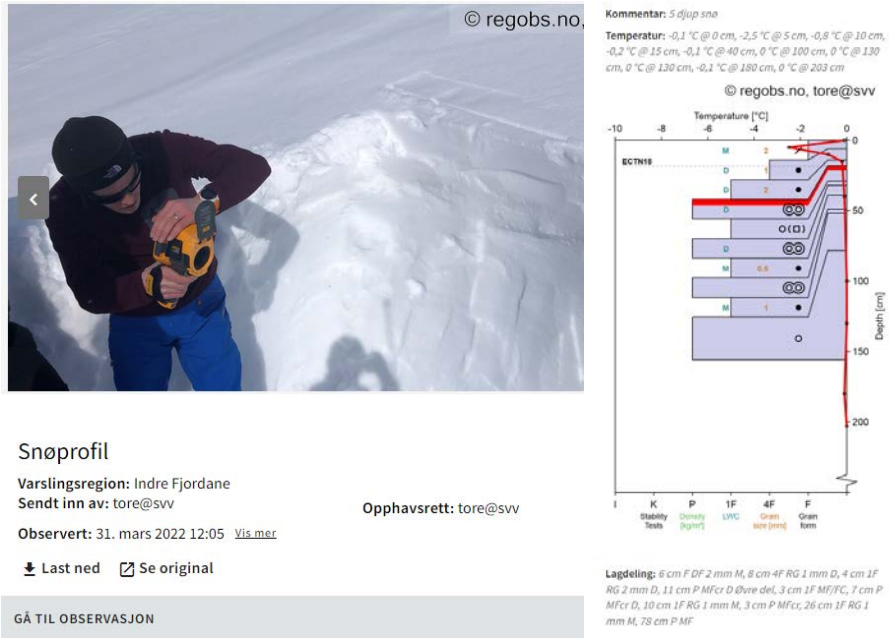

Figure 1-8. Example of a Varsom Regobs registered snow pit observation located close to Fonnbu; picture of thermal camera imaging in snow pit (left) and snow profile information (right), [https://regobs.no/registration/299587.](https://regobs.no/registration/299587)

1.4 Ground control points

Ground control points (GCPs) were placed in area A and B (Figure 1-5) for independent verification and correction of UAS-derived products (e.g. elevation maps). The GCPs consisted of 35 x 35 cm spray-painted fibreboard targets, attached to sticks for easy placement in the snow. The targets were deployed on the first field day and removed at the end of the last day. Target locations were measured 3-4 times over three days with an Emlid Reach RS2 handheld Real-time kinematic (RTK) GNSS receiver connected to the CPOS correction service from the Norwegian Mapping and Cadastre Authority (Statens kartverk). The precision of the GCP locations is given in Table 2-1. Slight changes in target locations during the period they were set out is not unlikely, but no indications of movement in specific directions were found.

Table 2-2. Precision of GCP observations, given by the standard deviation (SD) in each direction.

Area	Id	No. of observations	SD (x) [m]	SD (y) [m]	SD (z) [m]
A2	1	4	0.013	0.011	0.033
A2	2	4	0.012	0.007	0.035
A2	3	4	0.010	0.005	0.014
A2	4	4	0.017	0.018	0.032
A2	5	4	0.006	0.013	0.037
A2	6	4	0.009	0.014	0.055
B	1	3	0.014	0.007	0.071
B	2	3	0.013	0.027	0.041
B	3	3	0.010	0.023	0.011

2 Report from the Norwegian Public Roads Administration (NPRA)

2.1 Participants

From the Norwegian Public Roads Administration (NPRA), the following persons participated in the Fonnbu field test:

- Tore Humstad, engineering geologist, GEOSFAIR project manager
- Emil Solbakken, engineering geologist, WP4 leader
- Halgeir Dahle, engineering geologist, project adviser
- Dag Theodor Andreassen, geotechnical engineer, RPAS controller
- Jens Tveit, engineering geologist, on duty for site specific avalanche warning
- Torgeir Vaa, chief engineer and senior R&D adviser
- Edward McCormack, engineer and international adviser to GEOSFAIR

2.2 Preparations

NPRA was responsible for flight safety and flight coordination during the fieldwork. NPRA staff performed a general mission planning for UAS operations close to Fonnbu prior to the fieldwork. A Notice to Airmen (NOTAM) was issued to notify air traffic in the area about the operations. To streamline the fieldwork, it was necessary to facilitate simultaneous flights. In the preparations it was decided to coordinate the UAS operations using radio communication between the pilots and segregation of the airspace.

All UAS operations had to be performed within the “Open” category of the regulations for UAS. This restricted the operations to fly within visual line of sight (VLOS) and a maximum flight altitude of 120 meter above ground level.

NPRA was also responsible for avalanche safety for the field work. A map (Figure 1-2) describing potential release areas, runout zones as well as safe zones and critical points was developed and updated throughout the test week.

2.3 Work package addressed

NPRA is involved in all work packages, and in particular WP4 which is the integration of GEOSFAIR findings in the context of an enhanced decision support tool. The main NPRA activities at Fonnbu focussed on flights and use of different instruments, as well as manual snow investigations. NPRA activities supported the following work packages:

- Lidar and photogrammetry: WP1
- Use of Site Scan flight planning software: WP2 and WP4
- Snow investigations: WP1 and WP2

2.4 Goals prior to field testing

The main goals for the NPRA group were to:

- Perform repeated surveys with the DJI Zenmuse L1 lidar sensor mounted on a DJI Matrice 300 RTK drone to evaluate and document survey accuracy.
- Test the SiteScan software for flight planning, flight control and photogrammetric post-processing.
- Exchange knowledge and experiences about the different UAS currently used within the NPRA group.
- General support to and facilitation of field tests such as by completing snow observations and placing ground control points.

2.5 Field test activity

2.5.1 Lidar

Lidar data was collected in all test areas, and repeated lidar surveys were conducted for test areas A and B. All surveys were made with a DJI Zenmuse L1 sensor mounted on a DJI Matrice 300 RTK drone. Common survey parameters used for repeated surveys of areas A and B were: 60 m altitude above ground level (AGL) flight with terrain following enabled, 7 m/s flight speed, 50 % sideways overlap, and dual return mode. For all but one survey (area B, 30.03.2022), a repetitive scan pattern was used, and the sampling rate was varied between 240 000 and 120 000 pts/s.

After the flights, the data was pre-processed in the DJI Terra software. Further editing and validation of the point clouds was completed in ArcGIS Pro and CloudCompare software. An overview of the surveys of areas A and B, including resulting point density and vertical accuracy on GCPs, can be found in Table 2-2.

2.5.2 Photogrammetry

Image collection for photogrammetric processing was conducted in or around area A and area B with several different platforms:

- DJI Mavic 2 Pro
- DJI Phantom 4 RTK
- QuantumSystems Trinity F90+ with Sony RX1RII camera
- DJI Matrice 300 RTK with H20T thermal camera

Surveys with the Mavic 2 Pro platform were performed using SiteScan for every step from flight planning to inspection of finished surface models. The workflow was also tested by persons with little or no experience with photogrammetric mapping. Other surveys were planned and executed using other platforms and images were processed using Agisoft Metashape software.

2.5.3 Other

Other activities:

- Measurements of snow surface temperature to compare with thermal images collected with DJI H20T (airborne) and Fluke Ti-400 (handheld)
- Drone and pilot service for tests with GPR and multispectral camera
- Manual snow observations supporting tests with GPR and multispectral camera
- Preparation of ground control

2.6 Adjustments and lessons learned

No major adjustments were made during the field test. If more of the photogrammetric surveys had been processed immediately, the NPRA group would have discovered issues with low surface contrasts and GNSS positioning errors and tried to mitigate these.

Several issues were encountered when processing the photogrammetric surveys:

- Noise or non-matched images due to lack of recognisable surface features. This was expected for surveys that were carried out during flat light conditions or where the snow surface was covered with dry, new snow unaffected by wind. Incomplete image matching was however also experienced in cases where the images visually seem to contain more than enough surface contrast. The reason for this is unclear, but one theory is that direct sunlight in combination with high surface reflectivity (faceted snow) might have caused surface features to appear slightly different from different angles.
- GNSS position errors. One survey carried out with Trinity F90+ suffered from very large positioning errors during the first half of the flight, probably due to long time to first fix/too early take off. On the remote controller, only the number of satellites is shown and not the quality of the position solution. Conclusion is to wait for >30s before take-off after pre-flight check and to consider extending the flight route from take-off to start of survey.
- GNSS position errors 2. Two other photogrammetric surveys of area A2, one with P4 RTK and Trinity F90+, resulted in around 30 cm vertical RMS errors on GCPs. Mean vertical errors were -27 cm and 31 cm, respectively, and the two surveys were performed about an hour apart. These errors are much larger than what was previously experienced with the same systems. The exact causes are unknown, but poor satellite geometry and/or disturbance from GNSS signal reflection are suggested as possible issues.
- Low overlap over protruding terrain. Terrain undulations along flight strips can cause significantly lower flight altitude and thereby less image overlap in parts of the survey area. This issue gets worse the lower the resolution of the terrain following function is. Areas with several meters of snow must also be accounted for, if the terrain following function is using a snow-free terrain model.

Other:

- Manual classification of snow surface properties is difficult and dependent on the person doing the classification. Future collection of detailed snow surface data for calibration of multispectral signals should be based on established, instrument-based methods for snow grain classification.
- An easy way of retrieving coordinates for Regobs observations would be useful.
- Initial processing of survey data should ideally be done shortly after flight, to check data quality and to allow adjustments along the way.

2.7 Future activities

The test generated the need for the following future activities:

- Investigate different sources of GNSS positioning errors
- Streamline workflows and create checklists to ensure survey quality
- Test different opportunities for automated/semi-automated data flow, from sensor data to results presented in a web viewer
- Prepare use of optical instruments for snow grain classification

2.8 Preliminary Products

Figure 2-1 to Figure 2-4 below show a series of lidar-derived elevation products obtained during the test. In general, the lidar results provided accurate information about snow heights and about the nature of the snow surface.

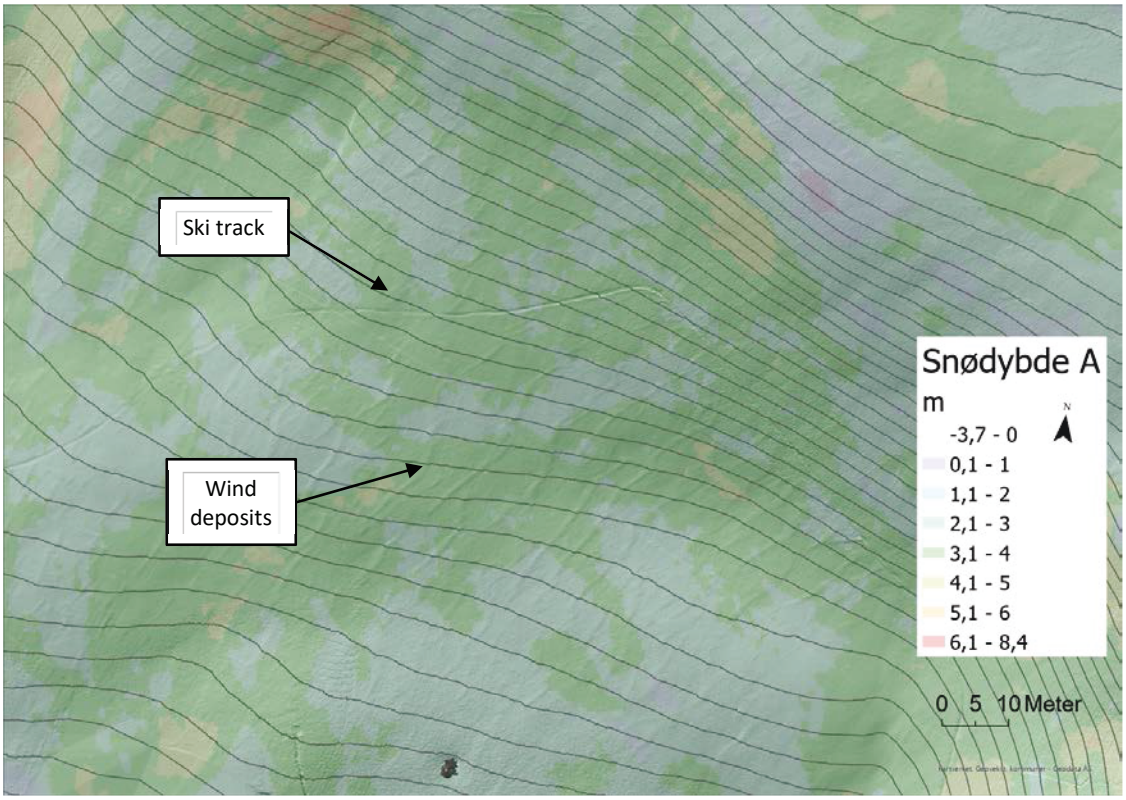

Figure 2-1. Snow height (Nor. 'snødybde') draped on hillshaded snow surface within test area A. Snow height estimates are made by comparing the lidar-derived measurements of the snow surface to the national elevation model. 1-m contour interval on the snow surface.

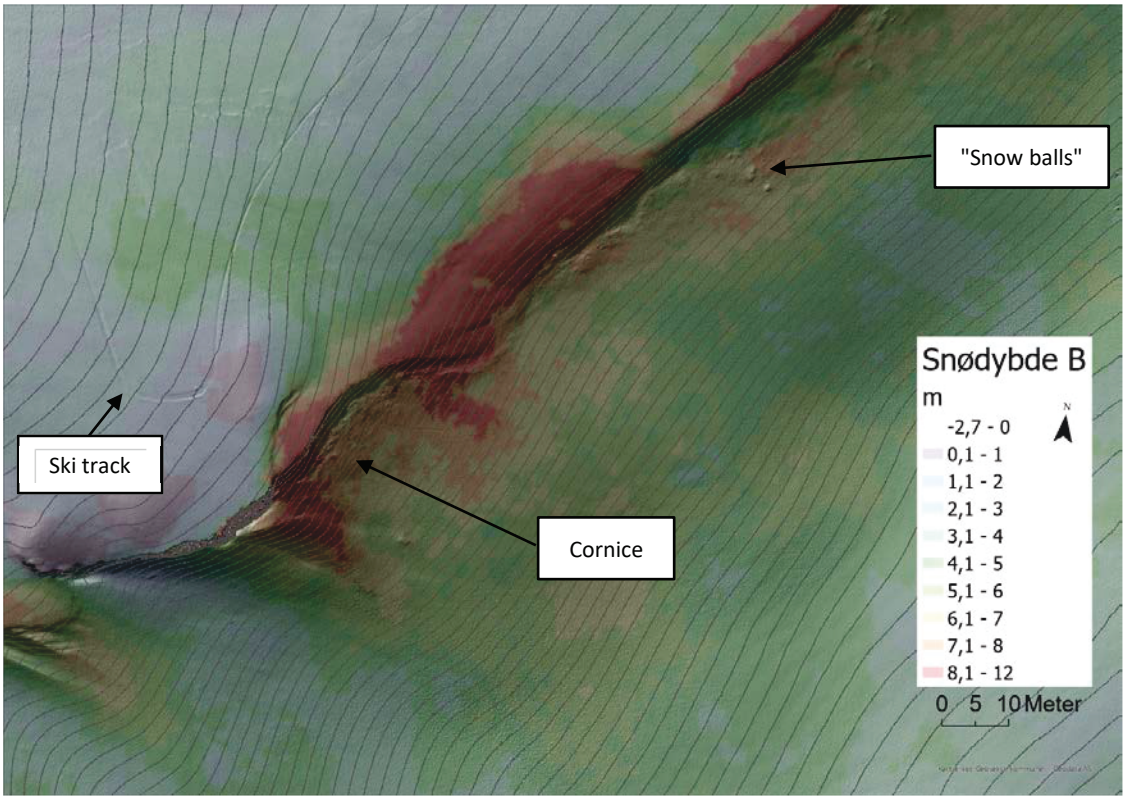

Figure 2-2. Snow height (Nor. 'snødybde') draped on hillshaded snow surface within test area B. Snow height estimates are made by comparing the lidar-derived measurements of the snow surface to the national elevation model. 1-m contour interval on the snow surface.

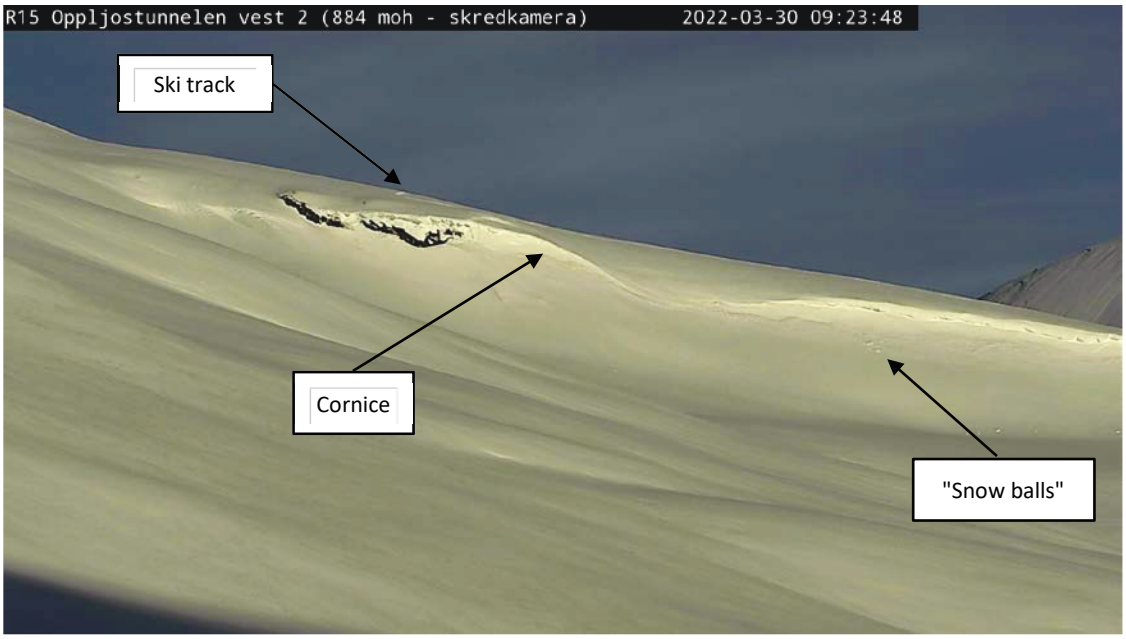

Figure 2-3: Photo of the same cornice mapped in Figure 2-2. The photo is taken with an automatic camera system at road Rv. 15. (Photo: NPRA, March 30, 2022)

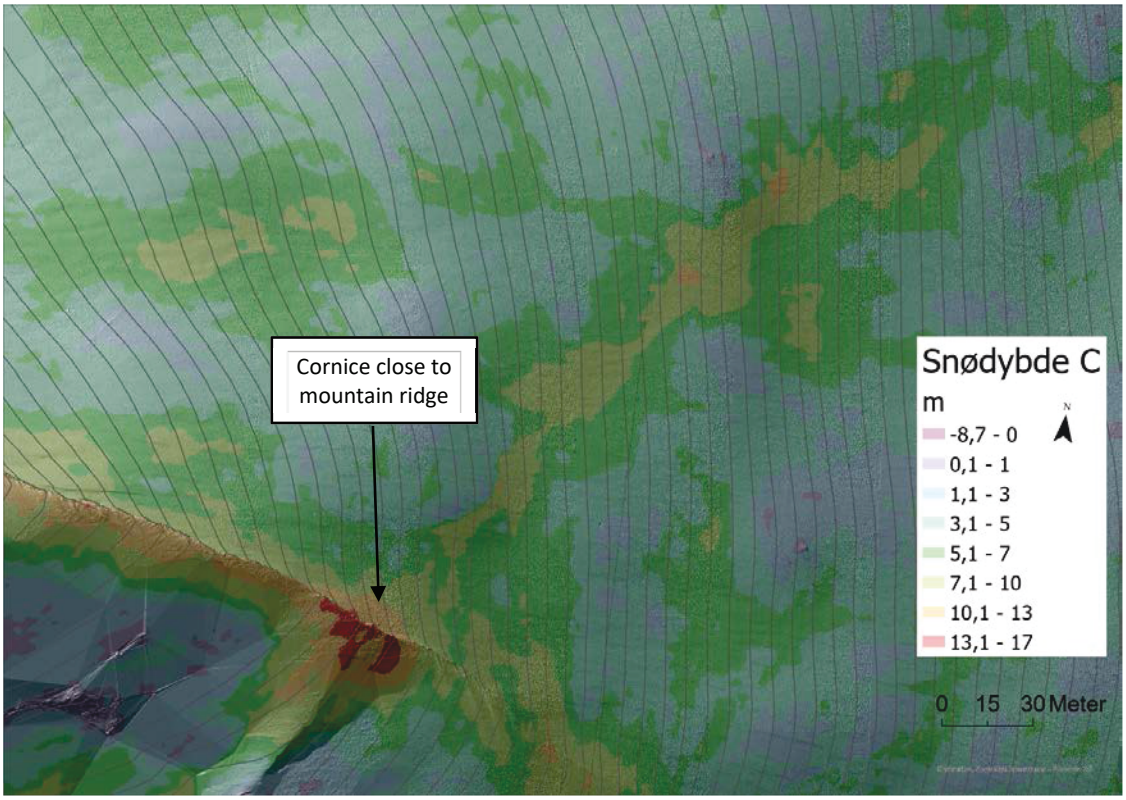

Figure 2-4. Snow height (Nor. 'snødybde') draped on hillshaded snow surface within test area C. Snow height estimates are made by comparing the lidar-derived measurements of the snow surface to the national elevation model. 5-m contour interval on the snow surface.

Figure 2-5: Photo of the same cornice mapped in Figure 2-4. The photo is taken with an automatic camera system at Kvitenova, 1400 m a.s.l. (Photo: NPRA, March 30, 2022)

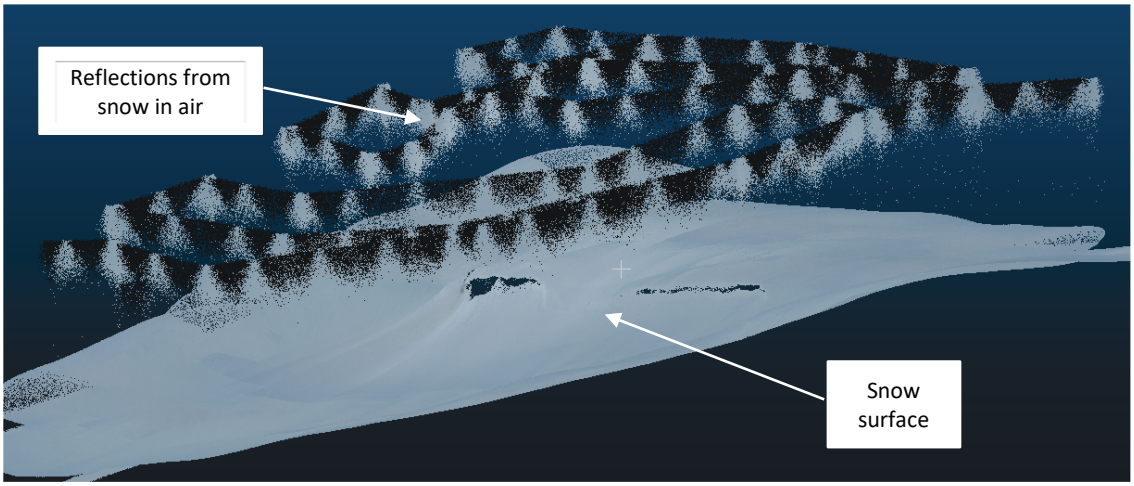

Figure 2-6. Lidar scanning during light snow showers at site B. The terrain surface is still detected, but there is considerable noise from reflections from air-suspended snowflakes.

Table 2-1. Overview of surface mapping surveys of areas A2 and B conducted by the NPRA. Survey accuracies are indicated by the root-mean-squared (RMS) and mean errors calculated on independent ground control points.

Area	Date	Time	UAS	Sensor	Flight altitude [m AGL]	Overlap, sidelap [%]	Sampling rate [pts/s]	Point density [pts/m2]	RMS error (z) [m]	Mean error (z) [m]
A2	30.3.2022	11:38	M300	L1	60	0, 50	240	1147	0.155	0.154
A2	30.3.2022	13:50	Trinity	Camera	100	85, 75			0.333	0.306
A2	30.3.2022	14:55	P4 RTK	Camera	70	85, 75			0.296	-0.272
A2	31.3.2022	15:17	M300	L1	60	0, 50	240	1096	0.052	0.012
A2	31.3.2022	15:25	M300	L1	60	0, 50	120	582	0.137	0.134
B	30.3.2022	12:01	M300	L1	60	0, 50	240	1082	0.098	0.096
B	31.3.2022	11:36	M300	L1	60	0, 50	240	1124	0.052	0.047
B	31.3.2022	14:15	M300	L1	60	0, 50	240	1312	0.098	0.098
B	31.3.2022	14:35	M300	L1	60	0, 50	120	653	0.153	0.153

3 Report from SINTEF Industry (Trondheim)

3.1 Participants

The SINTEF Industry group consisted of the following persons:

- Bastien Dupuy, research scientist, WP2 leader
- Arnt Grøver, research scientist
- Pauline Lorand, MSc student (SINTEF and Univ. Grenoble, France)

3.2 Work package addressed

SINTEF Industry is leading WP2 and is involved in WP1, WP3 and WP4. The activities carried out at Fonnbu were especially relevant for WP1 (Ground Penetrating Radar/GPR measurements) and WP2 (GPR processing, automatic flights following terrain, close to surface: 1–10 m for GPR surveys, and autonomous flights and data processing for photogrammetric surveys).

3.3 Goals prior to field testing

The goals for this field test were numerous and were mostly aimed at testing sensors (GPR) and data recording and processing routines. Specifically, the team planned to:

- Test GPR sensor using a Matrice 300 RTK platform on different sites with different snow thicknesses and determine layering (if possible). Test of flight altitude and speed.
- Test GPR sensor for rescue scenario including testing flying patterns to find buried targets (metal object or human).
- Test GPR sensor on the ground especially antenna angle versus slope angle.
- Test SnowScope probe to derive snow hardness profiles for correlation with GPR data.
- Conduct photogrammetric survey missions with SINTEF's GeoDrones Prototype 1 drone.

3.4 Field Test Activity

SINTEF's GPR system consists of a lightweight electromagnetic antenna with a central frequency of 1000 MHz and frequency band of 600 to 1300 MHz. With this frequency, it is theoretically possible to resolve ice layers of 1.7 cm at best with 5.7 cm being the minimum resolution. The resolution depends directly on the wavelength which itself is driven by frequency and wave velocity. Snow layers have a higher velocity than ice, so the resolution is less good, up to 2.8/9.3 cm for precipitation particles (lowest density i.e. lowest permittivity). These values are indicative and are calculated theoretically for best conditions and such optimal conditions are rarely met in field conditions.

In addition, the GPR system owned by SINTEF is not centred at 1000 MHz but at a lower frequency between 600 and 700 MHz. Theoretical resolution for ice layers is consequently between 2.6 and 8.7 cm and up to 14.3 cm for precipitation particles.

Figure 3-1 shows the GPR system (orange box) mounted on a DJI Matrice 300 RTK drone. The GPR antenna required connection with the onboard computer for data logging and georeferencing. Better data quality is achieved if the antenna is flown close to the snow surface, so it is recommended to be used with a radar altimeter allowing to follow the terrain accurately.

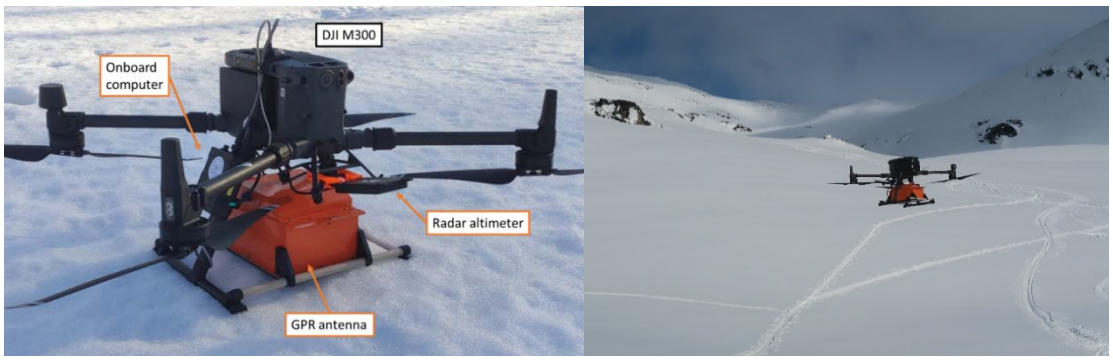

Figure 3-1. Left: GPR system mounted on drone and combined with onboard computer and radar altimeter. Right: in-flight measurements with GPR. (Photos: Tore Humstad)

First, repetitive UAS flights were carried out to optimize flight altitude. The goal was to find the best compromise between flight safety (flying as high as possible above ground/snow surface to avoid collisions) and GPR data quality. Data quality decreases rapidly when the antenna is far from the target due to the antenna radiation pattern and geometrical spreading of electromagnetic waves. Figure 3-2 shows examples of radargrams (2D GPR sections) of the same profile at different flight altitudes (1.5, 2.5 and 5 meters). On the 1.5 and 2.5 m altitude profiles, similar data quality was observed, where the diffraction hyperbola (likely due to boulders at ground surface) are well visible. The profile recorded at 5 m flight altitude are noisier and the data quality is affected. The conclusion is that flights between 2 and 3 m altitude are the best compromise.

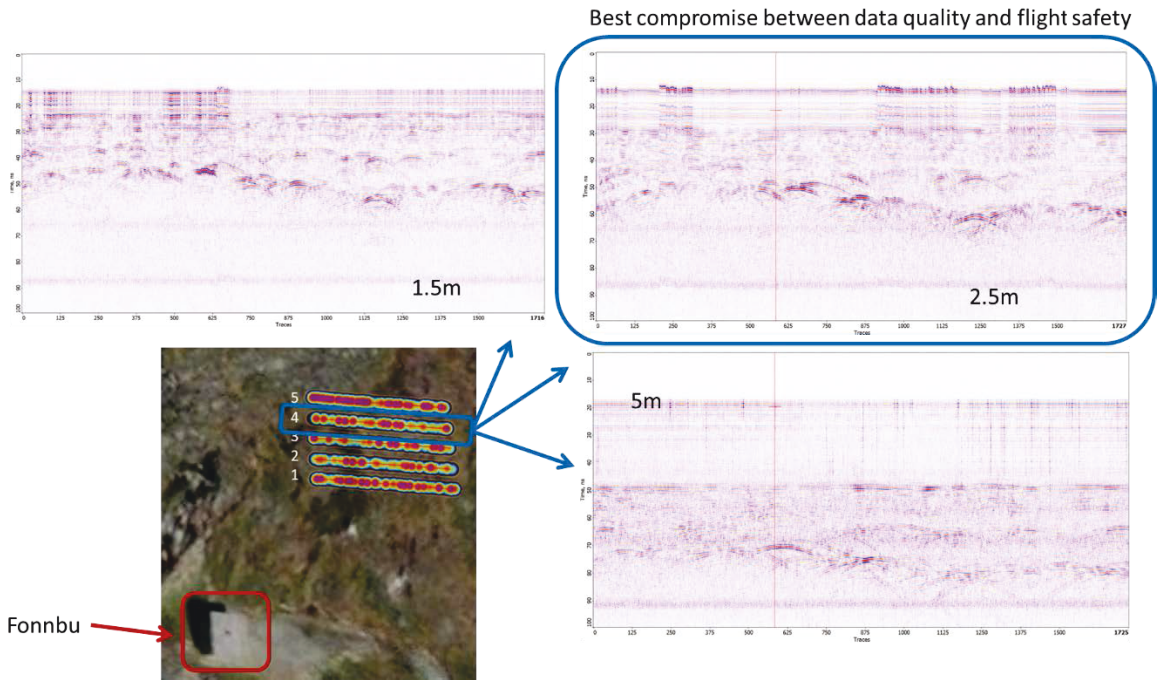

Figure 3-2. GPR cross-section radargrams. Test of different flight altitudes in area A1. Top left: 1.5 m UAS flight altitude above snow surface, top right: 2.5 m, bottom right: 5m. Bottom left: top view of GPR profiles location with respect to Fonnbu station. The 2D radargrams plotted here are extracted from profile 4.

The data presented in Figure 3-2 were recorded during a sunny and warm day and were successful. However, most of the time the team struggled with electronic failure of the GPR system due to cold weather. Recorded temperatures at the snow surface were around -5°C, and the GPR system is designed to handle -20 to +60°C internal temperature. But, as displayed in Figure 3-3, noise starts to appear after waypoint 2 and the full system completely stops working after waypoint 4. After several indoor and outdoor tests on site, it was concluded that the failure was due to the cold temperatures. After the field test, the GPR manufacturer acknowledged that the GPR system was not functioning correctly and that it will be repaired under warranty.

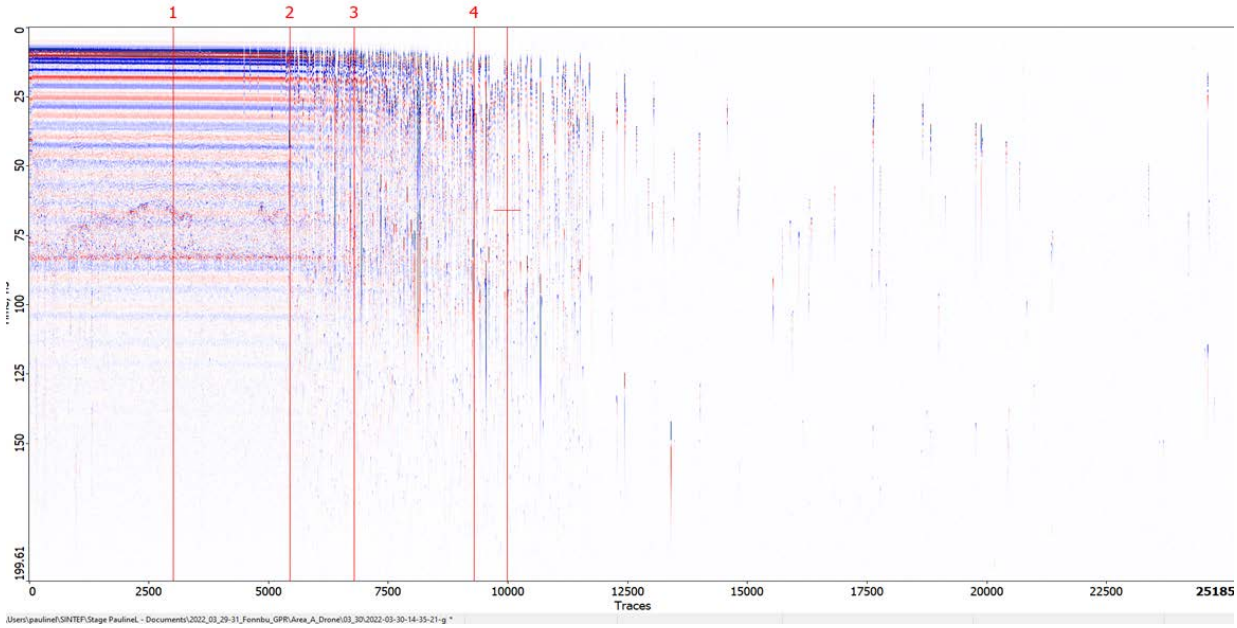

Figure 3-3. Example of GPR data where electronic failure in the system due to cold temperature leads to poor data quality. The red numbers 1, 2, 3 and 4 are waypoints in the UAS flying pattern. The displayed data is raw data prior to any processing.

To solve the cold temperature problem on site, the GPR antenna was insulated by wrapping it in a sleeping bag liner (see Figure 3-4). The GPR system worked better but unfortunately, the data was polluted by internal resonance due to wave reflections on this insulation layer.

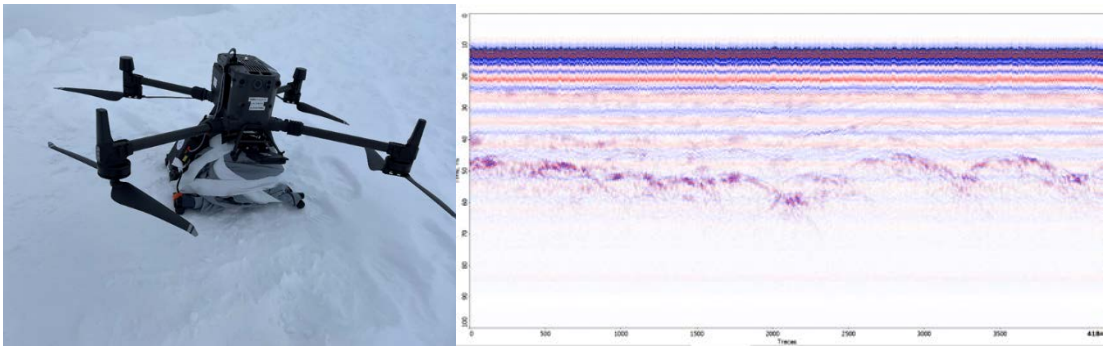

Figure 3-4. Left: custom-made solution to insulate GPR antenna. Right: example of recorded GPR data in this setting.

However, these tests were interesting in terms of UAS operations. The UAS was flown along the steeper slope (up to 20-22°) in test area A2 right above area A1 (see Figure 3-5). Both flights parallel to the slope and flights perpendicular to the slope were successful at low altitudes (down to 1.5 m). Flying upwards perpendicular to the slope was the most challenging as it required low enough flight speed (0.5 m/s) to allow the terrain-following algorithm to adapt based on radar altimeter measurements. A summary

of all the flights carried out during the field tests are given in Table 3-1 together with details on what was tested and whether it was successful.

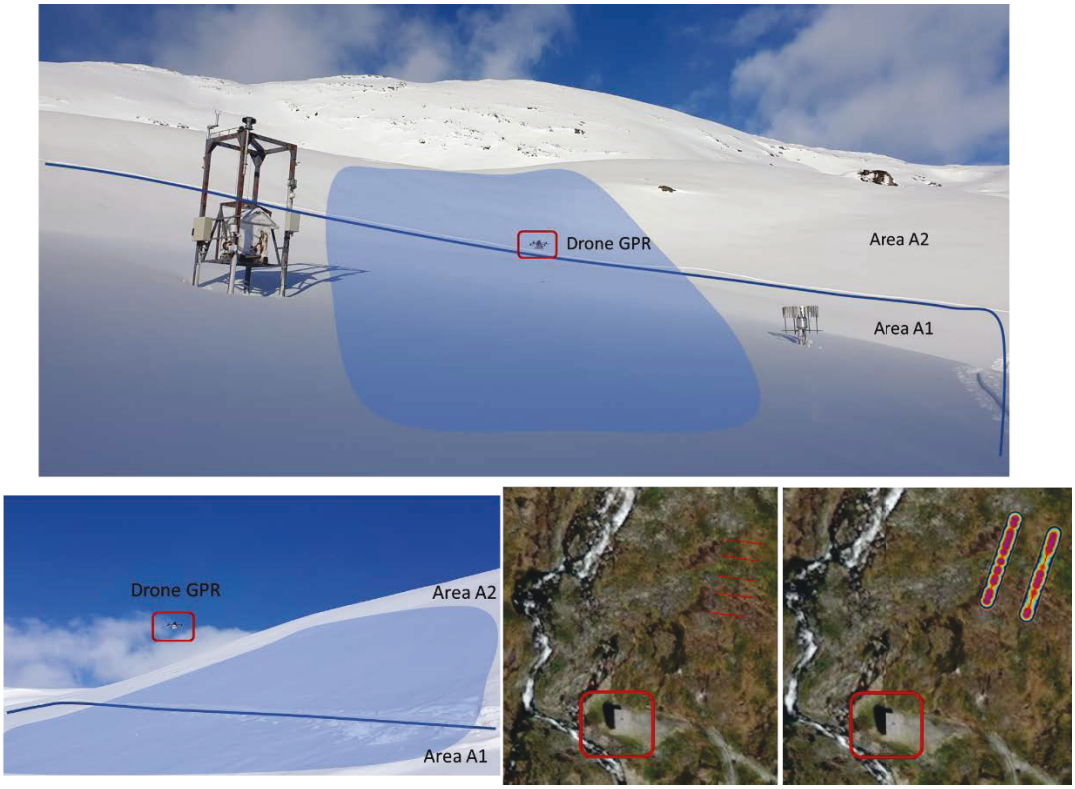

Figure 3-5. Pictures (top and bottom left) showing flight tests in steep terrain and flight patterns parallel (bottom center) and perpendicular (bottom right) to the slope for testing low altitude terrain-following flights and recording GPR data in a realistic steep mountain environment. In the pictures, the blue lines delineate test areas A1 and A2 (see map on Figure 1-3) and the blue area gives an approximate location of the survey in steep terrain. In the flight patterns figures, the red rectangles indicate the Fonnbu station location and the red (bottom center) and coloured (bottom right) lines represent the UAS flight patterns.

Table 3-1. Summary of all GPR surveys conducted during the field tests.

File name	Date	Time	Survey duration	Survey length	Location area	Flight altitude (m)	Flight speed (m/s)	Goal of survey	Data quality	Challenges
2022-03-29-14-38-13-gpr	29.mar				A1	Manual survey			Good	
2022-03-29-14-49-16-gpr				1 line	A1 + A2			Flight perpendicular to slope		
2022-03-29-14-54-09-gpr		14h54	-1 min	1 line						
2022-03-29-15-02-17-gpr				1 line						
2022-03-29-15-05-53-gpr		15h06	5 min	5 lines of 30 m	A1	2,5	1	Flight altitude		
2022-03-29-15-12-18-gpr						Manual survey				
2022-03-29-15-43-23-gpr				5 lines of 30 m		1,5	1	Flight altitude		
2022-03-29-15-54-16-gpr				5 lines of 30 m		5	1	Flight altitude		
2022-03-30-07-29-26-gpr	30.mar								Not working	Too cold
2022-03-30-08-37-57-gpr										
2022-03-30-08-51-33-gpr										
2022-03-30-08-56-27-gpr									Bad	
2022-03-30-09-02-02-gpr										
2022-03-30-13-42-00-gpr						2	1	Flight altitude		
						2,5	1			
						3	1			
						3,5	1			
						4	1			
						4,5	1			
						1	0,5			
2022-03-30-14-21-21-gpr					A1 + A2	5	1	Flight perpendicular to slope		
2022-03-30-14-27-48-gpr						5	1			
2022-03-30-14-35-21-gpr						5	1			
2022-03-30-14-51-35-gpr						5	1	Flight altitude, perpendicular to slope		
						4	1			
						3	1			
					A1	3	1	Flight altitude		
DAT_0001	30.mar				B	Ground/pulk			Good	
DAT_0002										
DAT_0003										
DAT_0004										
DAT_0005										
DAT_0006										
2022-03-31-09-29-11-gpr	31.mar				A1				Not working	GPR insulated (custom)
2022-03-31-09-32-46-gpr										
2022-03-31-09-40-32gpr										
2022-03-31-09-48-41-gpr		9h50	4 min	5 lines		4	1	Flight altitude	Average	
		9h56	4 min	5 lines		3	1			
		10h01	4 min	5 lines		2	1			
2022-03-31-10-12-12-gpr		10h13	4 min	2 lines	A1 + A2	4	0,5	Flight altitude, perpendicular to slope		
		10h18	4 min	2 lines		3	0,5			
		10h23	4 min	2 lines		2	0,5			

In addition to the UAS-borne GPR tests, the GPR instrument was also used directly on the snow surface. Specifically, the GPR was carried in a sled, from Fonnbu up towards test area B, passing by snow pit B-2 and up to snow pit B-1. Figure 3-6 shows the sled setup and the approximate location of the profiles. Six profiles were carried out, but their exact GNSS coordinates were approximated as only the starting and stopping points were recorded and the GNSS was not linked to the GPR in real time. Figure 3-7 shows the GPR profiles for these ground surveys. The interface between snow and ground is clearly visible and some internal layering can be observed as well.

Work is ongoing to process all the GPR data and to derive quantitative measures from the data i.e., snow height, snow properties and layering. This information can be correlated with snow pits and snow height maps derived from photogrammetry and lidar scans. Snow hardness profiles were also gathered using a PropagationLabs Snowscope probe. An example of a measured profile, as well as the location of measured profiles, is given in Figure 3-8. The goal of using this type of probe is to get ground truth measurements at several locations along the GPR profiles. The Snowscope probe derives hand hardness equivalent without the need for digging snow pits. The hardness can be

correlated to snow density and consequently to permittivity and GPR wave velocity, allowing for calibration of snow thickness estimations. However, the team experienced difficulties to operate the probe, especially Bluetooth connection challenges (the probe is connected to a phone app), and the probing was only successful (sometimes) in the upper part of the snowpack.

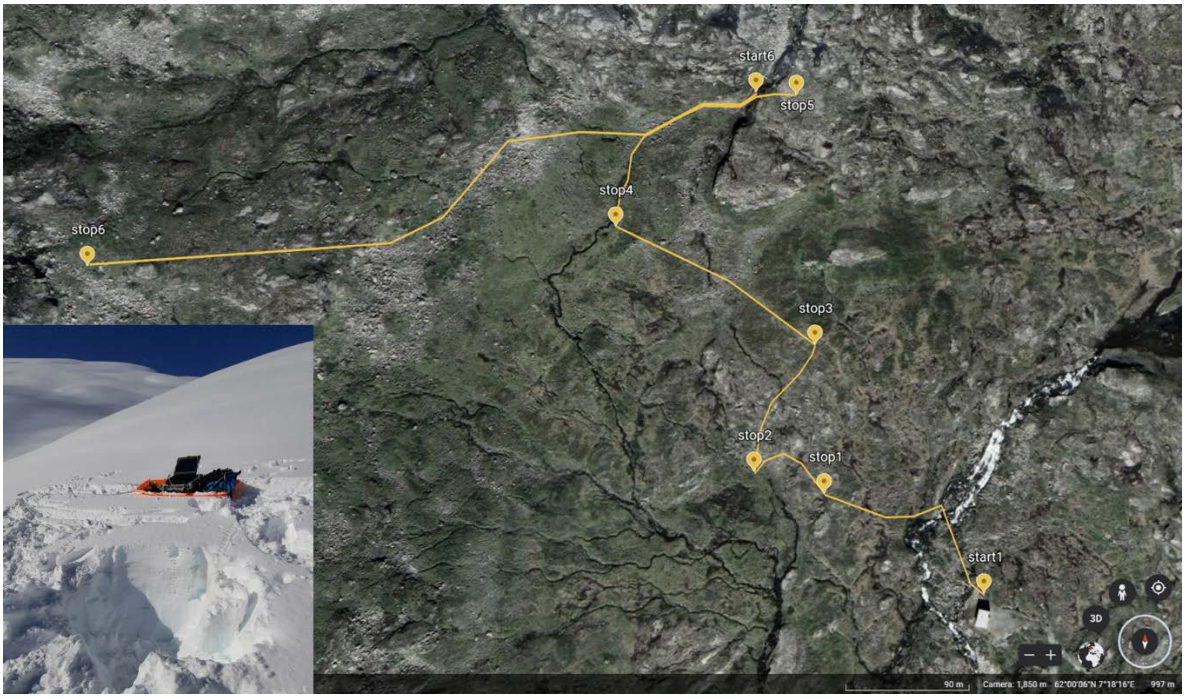

Figure 3-6. Ground (sled) GPR profiles. The profiles started at Fonnbu station (Start 1) and continued towards test area B (Stop 6). Stop 2 marked the location of snow pit B-2 and Stop 6 is the location of snow pit B-1.

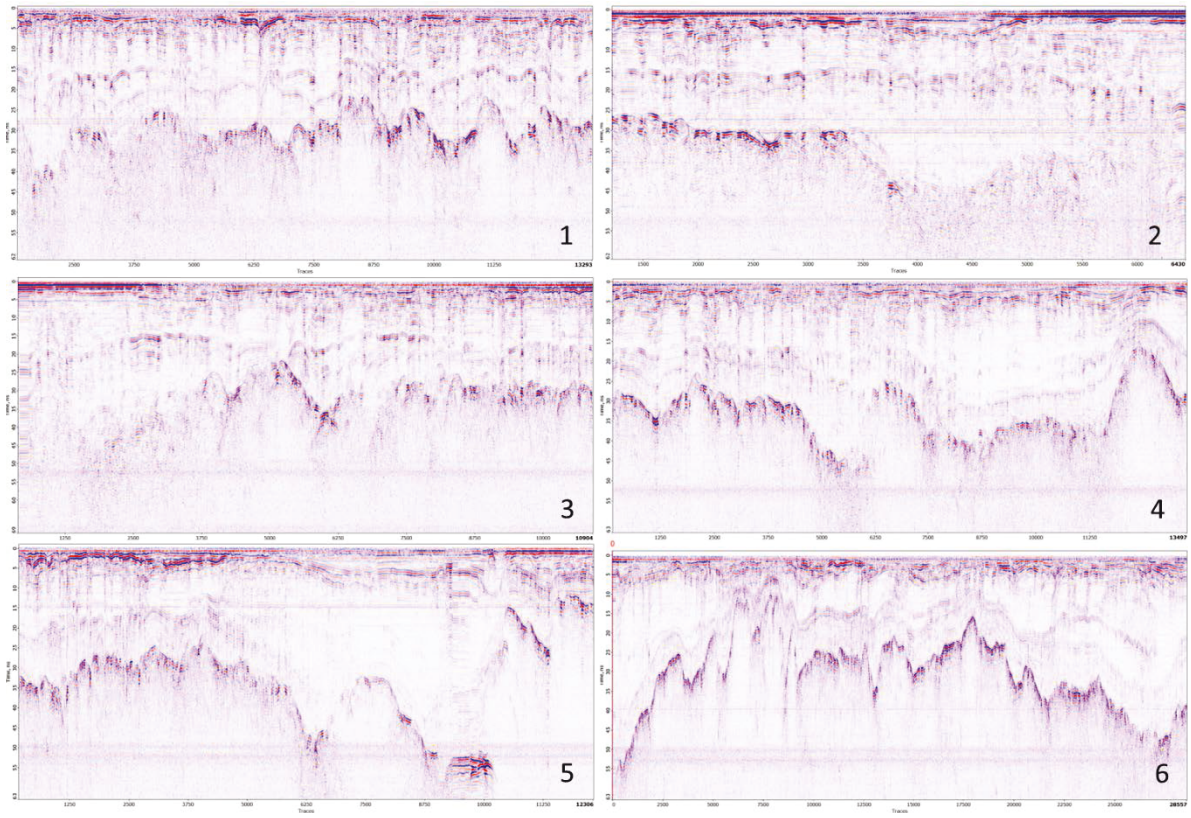

Figure 3-7. Ground (sled) GPR profiles. The profile numbers (1 to 6) correspond to surveys plotted in Figure 3-6. The end of profile 2 corresponds to snow pit B-2 and the end of profile 6 corresponds to snow pit B-1. Calibration of GPR data with ground truth from the snow pit will be completed, at least for the shallow layers.

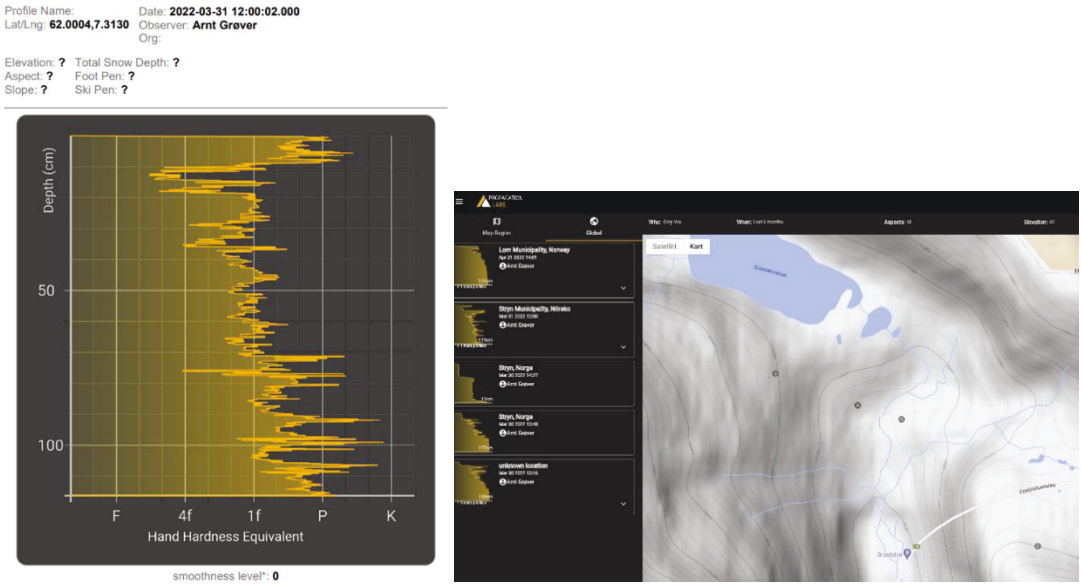

Figure 3-8. Example of Snowscope results (left) and location of probe profiles (right).

3.5 Adjustments and lessons learned

Photogrammetric surveys with SINTEF's GeoDrone Prototype 1 were not carried out because of the absence of a SINTEF UAS pilot. Tests of GPR for rescue were not carried out because of lack of time, due to the challenges with the operation of the GPR in cold weather. Several tests and adjustments (e.g. insulation of GPR sensor) were done to try to make the GPR sensor work in low temperatures. The main issue was related to the poor operation of the GPR sensor at low temperatures. As it has been acknowledged by the manufacturer that it was due to electronic failure and that the sensor will be repaired under warranty, we expect normal operation next winter when the sensor is fixed. The team also expects to implement GNSS referencing when using GPR on the ground to allow for easier processing of the data. At the time of writing of this report, this aspect is implemented and tested, and we can record geo-referenced GPR data on a sled.

3.6 Future activities

The team will continue to process GPR datasets and will develop an algorithm to determine snow thickness, layering and snow properties. This aspect is part of the ongoing work of Pauline Lorand's MSc thesis (Université Grenoble/SINTEF). The team expects to conduct additional tests of the airborne GPR sensor, especially in more complex terrain: steep mountainous terrain, over cornices, over glide cracks, over avalanche debris, etc.

The team will also continue to test the SINTEF GeoDrones Prototype 1 with different sensors including RGB camera for photogrammetry, thermal camera and multispectral camera. The data processing workflow set up for photogrammetry will continue to be tested operationally and will extend to other sensors. This workflow consists of an automatic processing workflow (including hardware and software components).

3.7 Preliminary Products

Figures 3-2, 3-4 and 3-7 in section 3.4 show examples of preliminary results extracted from GPR data. Additional work is needed for quantitative results including true snow layer thicknesses (validated) and estimation of properties (density, liquid water content).

4 Report from SINTEF Digital (Oslo)

4.1 Participants

The SINTEF Digital group consisted of the following persons:

- Richard Moore, senior scientist
- Asbjørn Berge, senior scientist
- Trine Kirkhus, senior scientist (not present at Fonnbu, back-office)

4.2 Work package addressed

SINTEF Digital is leading WP 1. The aim of the field tests was to evaluate an imaging spectrometer as a means for remotely determining snow grain size based on the gradient in the red-edge and NIR part of the spectrum. The sensor tested was a MicaSense RedEdge-MX spectral camera.

Carrying a spectral camera on a UAS may enable determination of snow surface type over large area. This information may be collected multiple times during a winter season and could be used to build a model of the layers in the snowpack. The MicaSense RedEdge-MX camera is UAS flight ready and was primarily developed for precision agriculture applications.

4.3 Goals prior to field testing

The team set out to test the MicaSense RedEdge MX spectral camera, with a single camera (5 channels), and a dual camera setup (with 5+5 channels) to discriminate between snow types. The MicaSense camera is compatible with DJI drones e.g., the DJI Matrice 300 RTKthat was used during the tests.

The team wanted to test the spectral camera when flying over larger areas and in local, controlled test sites where the snow type(s) was known. As the sensor data was captured under natural illumination, it was also desirable to capture data under various sun and slope angle conditions, to evaluate the effects of those parameters.

According to the manufacturer's specifications[5], the camera channel characteristics are listed in Table 4-1 and Table 4-2.

[5] https://support.micasense.com/hc/en-us/articles/214878778-What-is-the-center-wavelength-and-bandwidth-of-each-filter-for-MicaSense-sensors-

Table 4-1. Channel specifications for RedEdge-MX with serial numbers RX02 or higher ('Red' camera).

File suffix	Band name	Center wavelength (nm)	Bandwidth (nm)
1	Blue	475	32
2	Green	560	27
3	Red	668	14
5	Red Edge	717	12
4	Near IR	842	57

Table 4-2. Channel specifications for RedEdge-MX 'Blue' (in the Dual Camera System):

File suffix	Band name	Center wavelength (nm)	Bandwidth (nm)
6	Coastal Blue	444	28
7	Green	531	14
8	Red	650	16
9	Red Edge	705	10
10	Red Edge	740	18

4.4 Field Test Activity

4.4.1 Handheld multispectral images of snow surface

Handheld multispectral images of the snow surface were captured at test sites A2-1, A2-2, A2-3 and A2-4 (Figure 1-5). Measurements at these four sites were repeated on Day 1 and Day 2 (Table 1-1).

At each test site, multiple image sets (each set containing 10 images from each spectral band) were captured from directly above the snow surface, at an angle of approx. 30° from normal pointing away from the sun, and at an angle of approx. 30° from normal pointing towards the sun. Each spectral camera was allowed to automatically adjust the exposure time. This effect was calibrated for in post-processing of the data.

Site A2-1 was visited on Day 1 afternoon, Day 2 morning, and Day 2 afternoon. Sites A2-2, A2-3, and A2-4 were visited on Day 1 afternoon and Day 2 morning.

- Day 1 afternoon had fresh snow with late sun.
- Day 2 morning had partially wind-affected snow with early sun.
- Day 2 afternoon had day-old snow with same sun angle as Day 1 afternoon.

This combination of tests should allow for the separation of the effects of sun angle, ground slope, and snow type on the captured sensor data.

4.4.2 Handheld multispectral images of snow height profile

Handheld multispectral images of the snow height profile were captured at test sites B1, B2 (Figure 1-5). Images were captured of the snow profile to investigate the visibility of the sub-surface layering in multispectral imagery. Although it is not proposed to

image sub-surface snow layers with this camera during deployment, the sub-surface layers may enable a wider range of snow types to be captured under identical imaging conditions – useful for analysing the discriminatory power of the proposed approach.

4.4.3 Airborne multispectral images of snow surface

UAS-mounted multispectral images of the snow surface were captured over test area A1 (see Figure 1-3) at approx. 20 m above ground level. Airborne imagery enabled the team to test a remote sensing deployment workflow, by processing captured imagery with Pix4DFields to visualise several standard agricultural metrics. Although these metrics are not optimal for discriminating snow types, they enabled the team to prove out the workflow for collecting and processing the image data.

Figure 4-1. The MicaSense multispectral camera mounted on NPRA's DJI Matrice 300 RTK aircraft. An external GNSS receiver was also mounted on the UAS for geotagging multispectral data. The camera was controlled directly from the ground via a WiFi interface. (Photo: Tore Humstad)

4.5 Adjustments and lessons learned

Although testing was carried out as planned, extensive post-processing was required on the captured test data. Camera-specific calibrations (using data provided in the metadata of the image files) and on site/illumination calibrations were required before data capture. This resulted in limited possibilities to quality control and inspect the data while in the field at Fonnbu.

4.6 Future activities

How to parameterize the snow types efficiently to use for making models? It is difficult to determine whether there was a large enough spread in snow types to determine how the spectral data could help to discriminate between snow types. Identifying which factors influence the data other than snow type, e.g., terrain inclination angle, sun's incident angle and characterising their effect/s will be an important outcome of analysis of the data captured at Fonnbu. Ideally, we wish to remove the effects of all other parameters other than the snow type. Future work will include developing a modular sensor package and analysis pipeline that will enable simpler data capture and in-field validation and inspection of captured data.

4.7 Preliminary products

The dataset consists of ten image files per photo capture. One image representing one wavelength. Examples below depict snow and the calibration board.

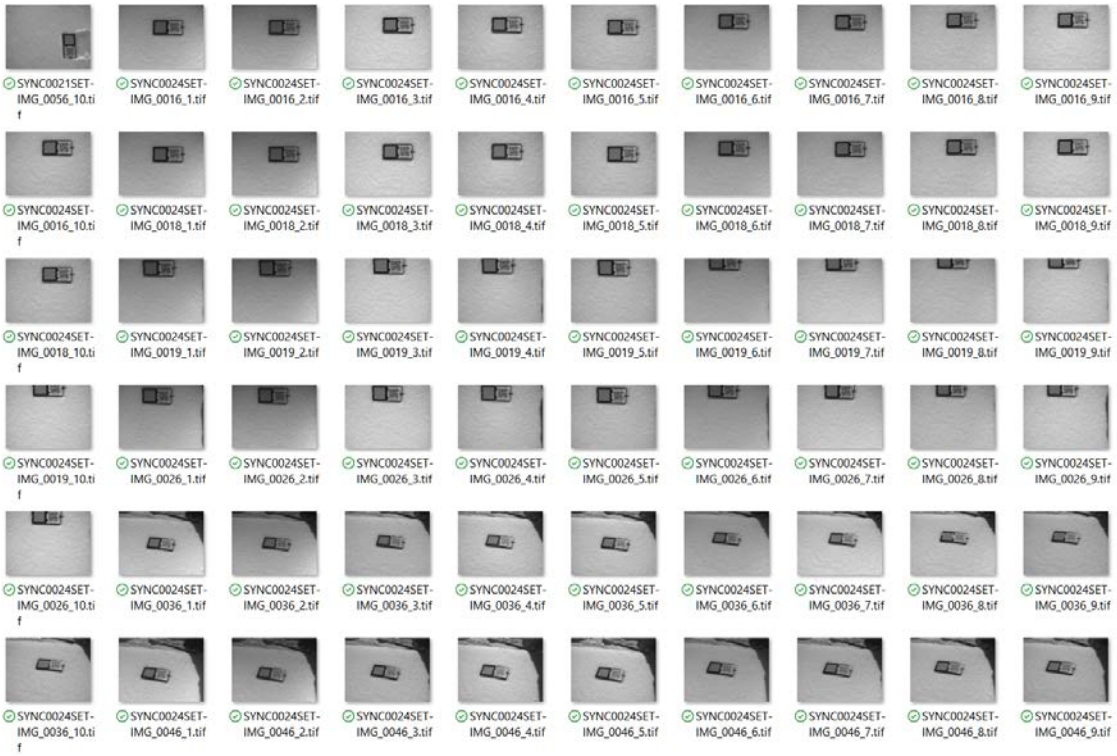

Figure 4-2. Spectral band images captured using MicaSense RedEdge-MX dual camera. Six photo captures produce 60 image files.

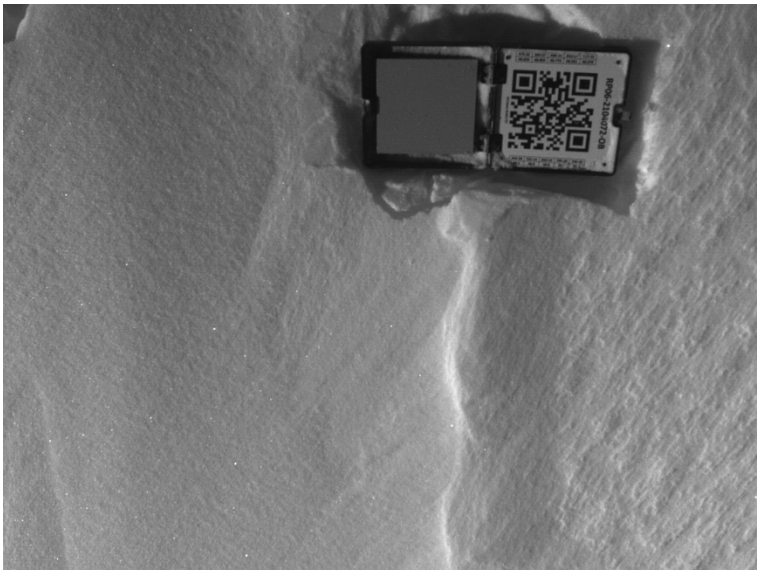

Figure 4-3. Example image of two snow types at test area A2-1 (regobs 305388). More wind affected snow at the right than in the left part of the image where there is wind slab. SYNC0052SET-IMG_0120_2.tif.

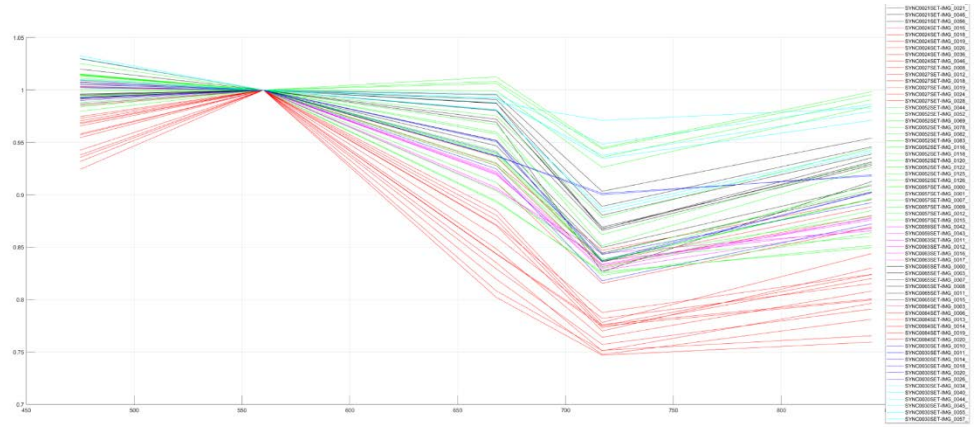

Figure 4-4. Sun angle effect on the RedEdge 'Red' camera. The colours represent the different sun angle vs terrain inclinations present during the tests.

Figure 4-5 and Figure 4-6 below depict a summary of the processed raw data for all handheld captures around test area A2. There were similarities between spectra captured under similar conditions, which validates to a degree the data captured. Specifically, first four spectra in the upper row represent the same snow type and terrain under direct sun and full shade and are mostly identical, which validates the goodness of our method for characterising incident illumination. For data captured at Fonnbu, this was achieved by means of a calibration board with calibrated reflectance. Similarly, spectra in the middle rows of the figure correspond to wind affected snow captured on Day 2 and have different forms to spectra captured in the upper and lower rows. Differences in snow surface texture are also visible in the reflectance images (Figure 4-5). The team is

continuing to characterise these differences to determine to which extent they correspond to actual differences in snow type.

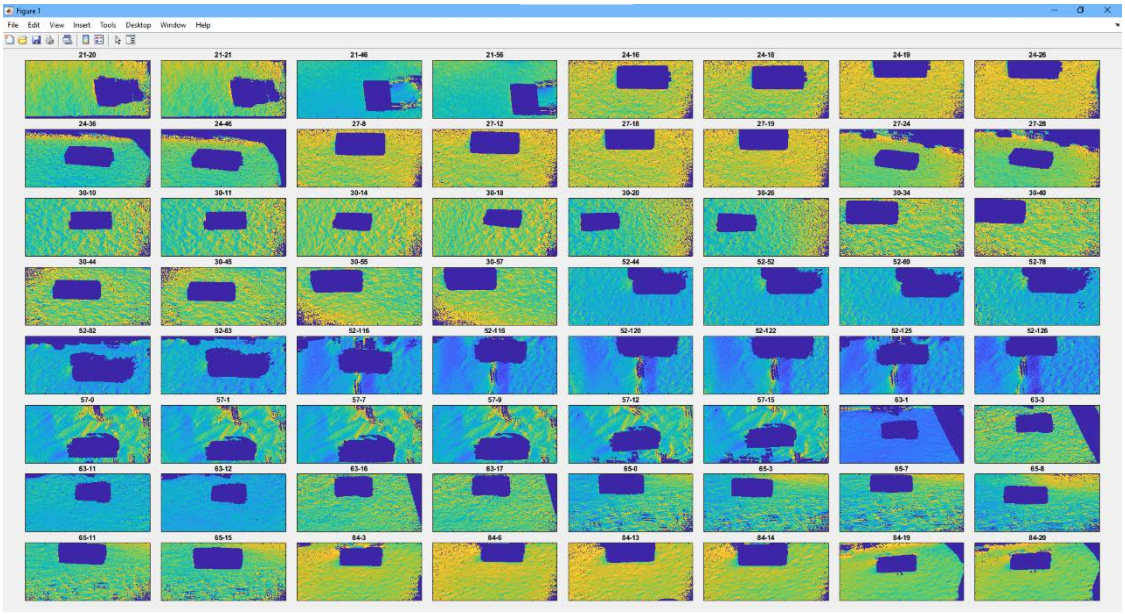

Figure 4-5. Example reflectance images (spectral band 5) from different test sites and conditions in test area A2. The calibration board and shadowed regions have been masked out, and remaining pixels scaled to enhance variations in snow surface texture.

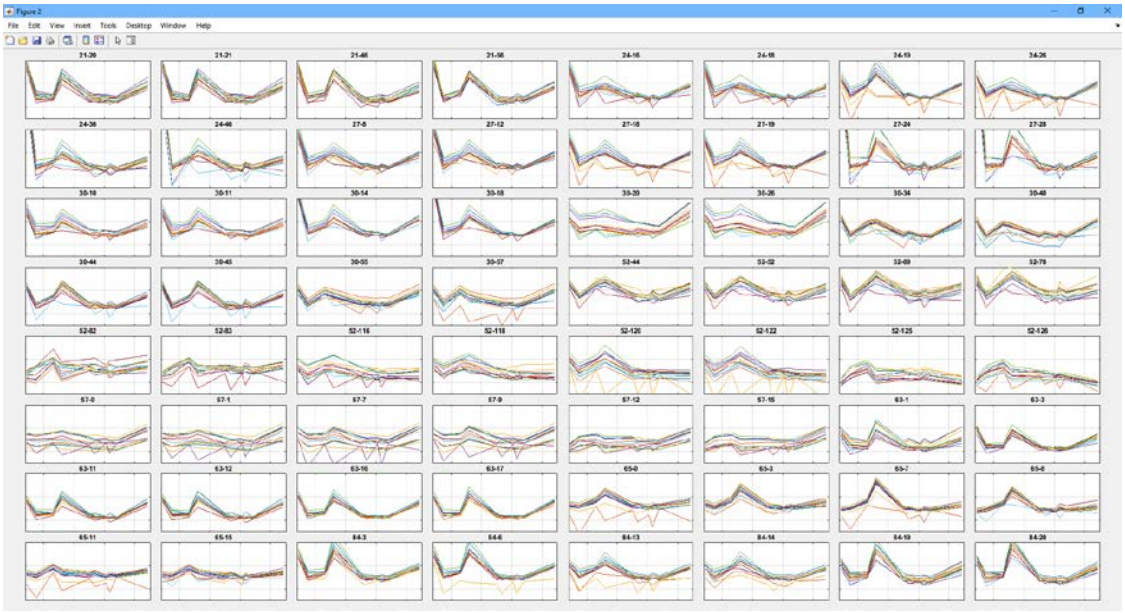

Figure 4-6. Spectra for test locations and conditions corresponding to reflectance images in above figure. Multiple lines in each set of spectra correspond to subregions within each image.

In the following figures, UAS-derived data products processed with Pix4D software is represented. The data were inspected immediately following data collection, while at Fonnbu and the image metadata was used to automatically process the image geometry and calibrate the radiation values.

Figure 4-7. UAS flight lines and image locations placed in Google Maps using Pix4D.

Figure 4-8. Colour images stitched together using Pix4D.

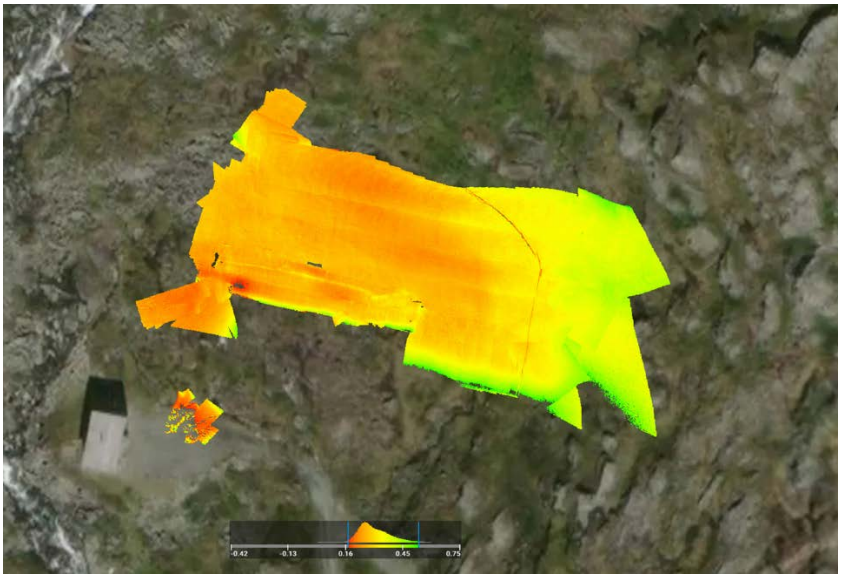

Figure 4-9. From Pix4D the MCARI-Index = ((VNIR - Red)-0.2(VNIR - Green))*(VNIR / Red) using Sentinel-2 Band 5 (VNIR), Band 4 (Red) and Band 3 (Green).*

5 Report from NGI

5.1 Participants

The NGI group consisted of the following persons:

- Regula Frauenfelder, technical expert, WP3 leader
- Sean Salazar, senior engineer
- Sunniva Skuset, project engineer (not present at Fonnbu, logistics/back-office)

5.2 Work package addressed

The NGI group organised and was responsible for all logistical aspects of the field test at NGI's avalanche research station Fonnbu (Figure 1-1), in the Strynefjellet mountain area. In cooperation with NPRA, NGI was also responsible for avalanche safety precautions.

NGI's contribution within WP3 supported interactions between the technology-based activities in WP1 and WP2 and the integration and uptake of UAS and UAS-derived data in WP4. In addition, the project group tested its own UAS, while also collecting ground truth and validation data.

5.3 Goals prior to field testing

UAS sensor data should be evaluated in terms of utility and validated by data collected using conventional instrumentation and hand-dug snow pits by avalanche experts from the NPRA and NGI. The outcome of this evaluation is important to assessing the feasibility of UAS-obtained results for implementation at the NPRA and integration into decision-making processes. This task is the crucial link between the WP1 and WP2 activities and the WP4 activity, thereby ensuring direct collaboration between technologists and decision makers.

5.4 Field test activity

The following field test activities were performed during the test week and are described in more detail in the subsequent subsections:

- UAS surveys using GNSS (satellite positioning only) and RTK positioning (using NTRIP virtual base station connection, rather than DJI-supplied local base station).
- Testing of FLIR Vue Pro R thermal camera with UAS gimbal.
- Snow pack characterization through snow pit analyses.
- Temperature-calibrated thermal imaging on snow using Fluke Ti-400 series hand-held camera.

5.4.1 UAS surveys

Multiple surveys were performed with the DJI Phantom RTK drone on each of the three full days at the station, 29/03 – 31/03 to cover all of the test areas and to test the quality of image acquisitions under different light conditions. Generally, light conditions were extremely bright and even with optimized camera settings (low ISO setting, smallest aperture opening, fast shutter speed), image exposure and fresh snow (uniform, little texture) resulted in poor Structure-from-Motion reconstructions. The relevant specifications of the integrated UAS camera are presented in Table 5-1.

Table 5-1. Specifications for integrated UAS camera (according to manufacturer specifications).

Sensor	1 inch CMOS Effective pixels: 20M
Lens	FOV 84°; 8.8 mm / 24 mm f/2.8 – f/11, auto focus
ISO range (Photo)	100–3200 (Auto) 100-12800 (Manual)
Mechanical Shutter Speed (Global Shutter)	8 – 1/2000 seconds
Max Image Size	4864x3648 (4:3 ratio) 5472x3648 (3:2 ratio)

Two major types of survey missions were conducted, including altitude-locked, double-gridline missions and terrain-following (altitude varying) missions, as illustrated in Figure 5-1. All missions were planned and executed using the native DJI GS RTK app on the aircraft controller (depicted in Figure 5-2). Terrain-following missions required the preparation of digital elevation models beforehand (uploaded to the controller memory) to maintain a constant ground sampling distance within images. In addition, a KML file delineating each of the test areas was used to assist in the flight mission planning, as labelled in Figure 1-3.

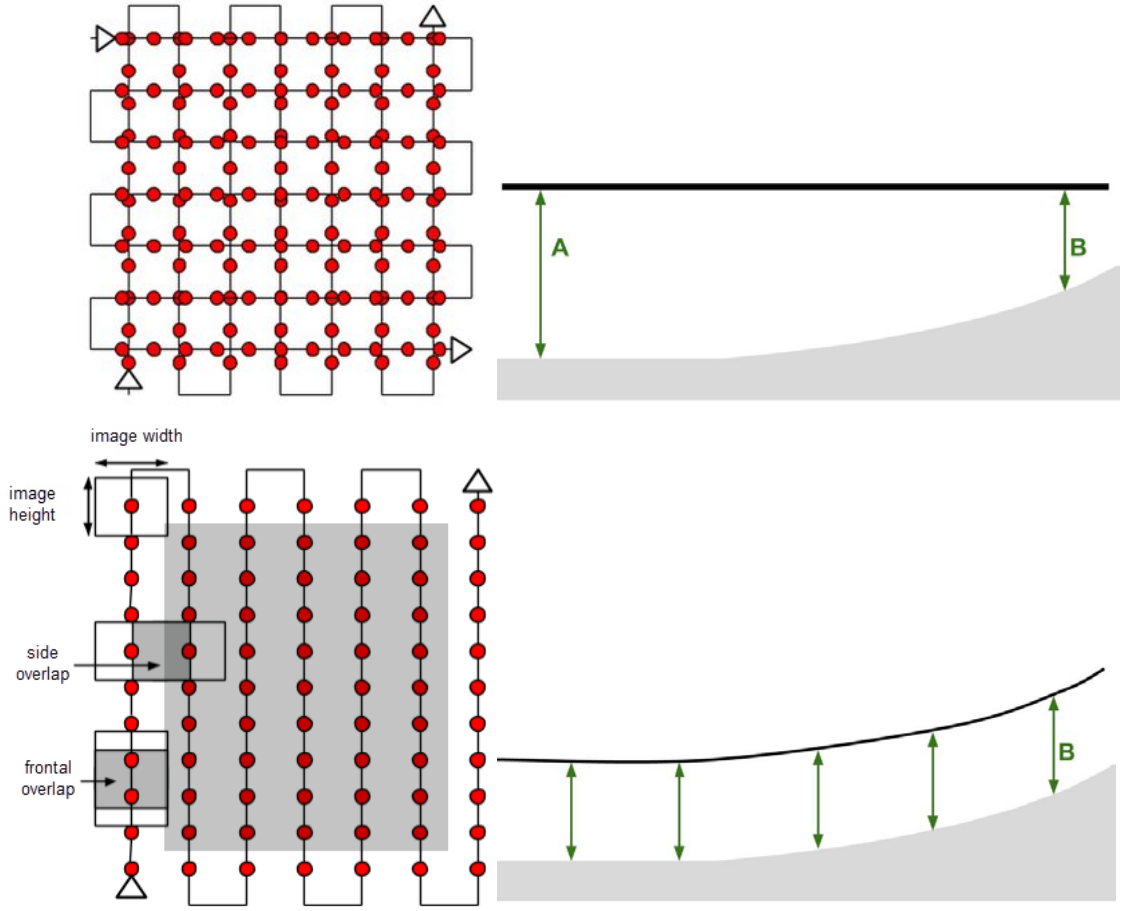

Figure 5-1. Typical flight pattern illustrations for double-gridline with constant altitude (top, top-down and profile views) and terrain-following (bottom, top-down and profile views) missions. Sources: Röder et al. 2017, Pix4D, Aerotas.

Figure 5-2. DJI flight controller used for planning and executing flight missions in the field. (Photo: Sean Salazar)

To measure the effects of aircraft positioning and the use of ground control on survey accuracy, flights were conducted using GNSS and RTK positioning, constant altitude and terrain-following modes, and using various control point configurations during photogrammetric processing. Ground control points were distributed within test areas A and B (labelled in Figure 1-3) and their locations were measured using a portable differential GNSS measurement unit. Test area C did not use ground control.

Effect of ground control

A GNSS-only flight using a constant altitude was conducted over area A to test a realistic scenario that used only limited planning and navigation tools. A total of 309 images were analysed using the Agisoft Metashape Structure-from-Motion photogrammetric processing workflow to perform alignment using either a single or two controlling GCP, as illustrated in Figure 5-3 and Figure 5-4. The resulting root-mean-square error (RMSE) values are presented in Table 5-2 and Table 5-3. The results indicated that adding one additional controlling GCP beyond the minimum improved the accuracy of the check points in the model by an order of magnitude. Additionally, an RTK-enabled, terrain-following flight was conducted over test area B. A single controlling GCP was used in the alignment, while the remaining two GCP were used as check points, as illustrated in Figure 5-5 and Figure 5-6. The resulting RMSE values are presented in Table 5-4 and Table 5-5, indicating the effect of GCP selection on the accuracy of the model. While direct comparison between survey methodology was not possible over the same test area, a comparison of the flights over test areas A and B indicated that the accuracy of the model generated from the RTK-enabled, terrain-following flight was improved by an order of magnitude over the model derived from the GNSS-only, constant altitude flight.

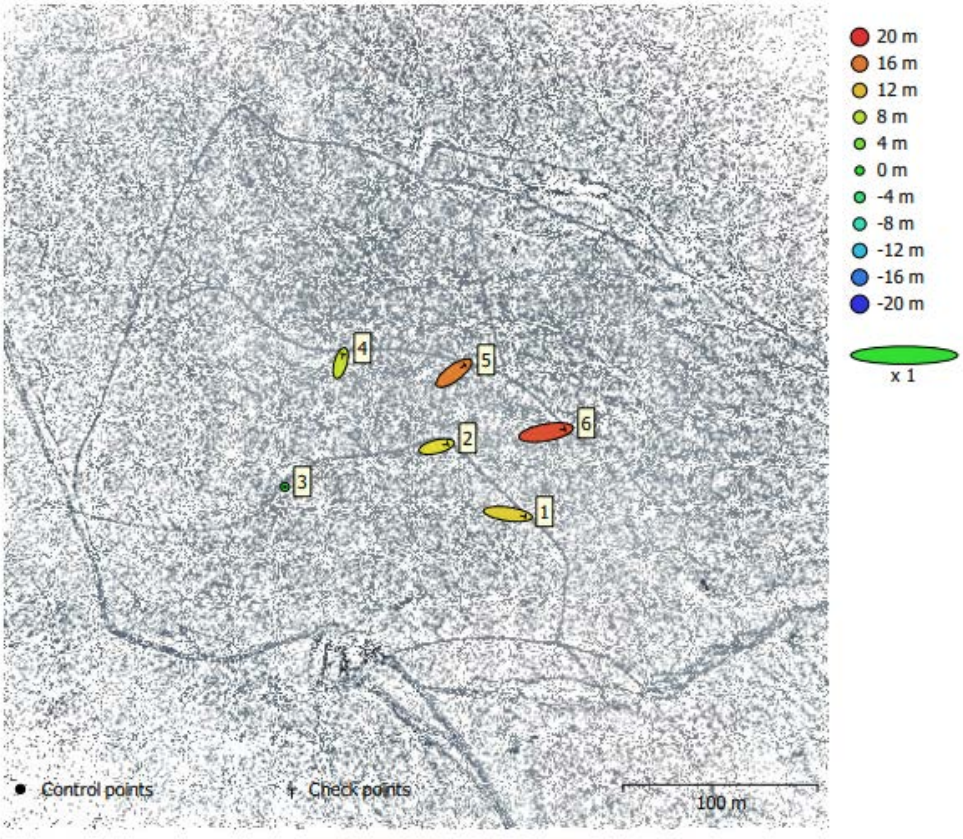

Figure 5-3. Photogrammetric reconstruction (sparse point cloud depicted) over test area A with ground control point (GCP) locations marked; GCP 3 used for bundle adjustment control while remaining five GCP used as check points.

Table 5-2. Control and check point RMSE, using a single control point (see Figure 5-3).

Count	X error (cm)	Y error (cm)	Z error (cm)	XY error (cm)	Total (cm)
1 (Control)	0.0153	0.00902	0.123	0.018	0.125
5 (Check)	1388	611	1324	1516	2013

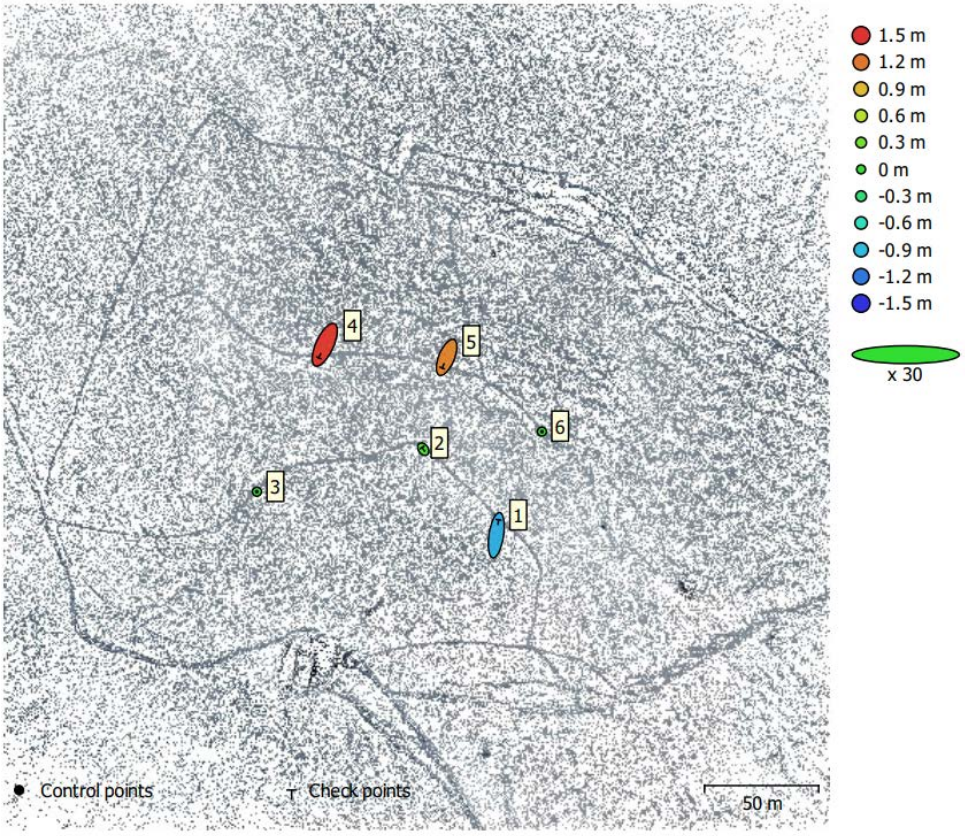

Figure 5-4. Photogrammetric reconstruction (sparse point cloud depicted) over test area A with ground control point (GCP) locations marked; GCP 3 and GCP 6 used for bundle adjustment control while remaining 4 GCP used as check points.

Table 5-3. Control and check point RMSE, using two control points (see Figure 5-4).

Count	X error (cm)	Y error (cm)	Z error (cm)	XY error (cm)	Total (cm)
2 (Control)	0.303	0.0625	0.189	0.310	0.363
4 (Check)	11.5	33.6	104	35.5	110.3

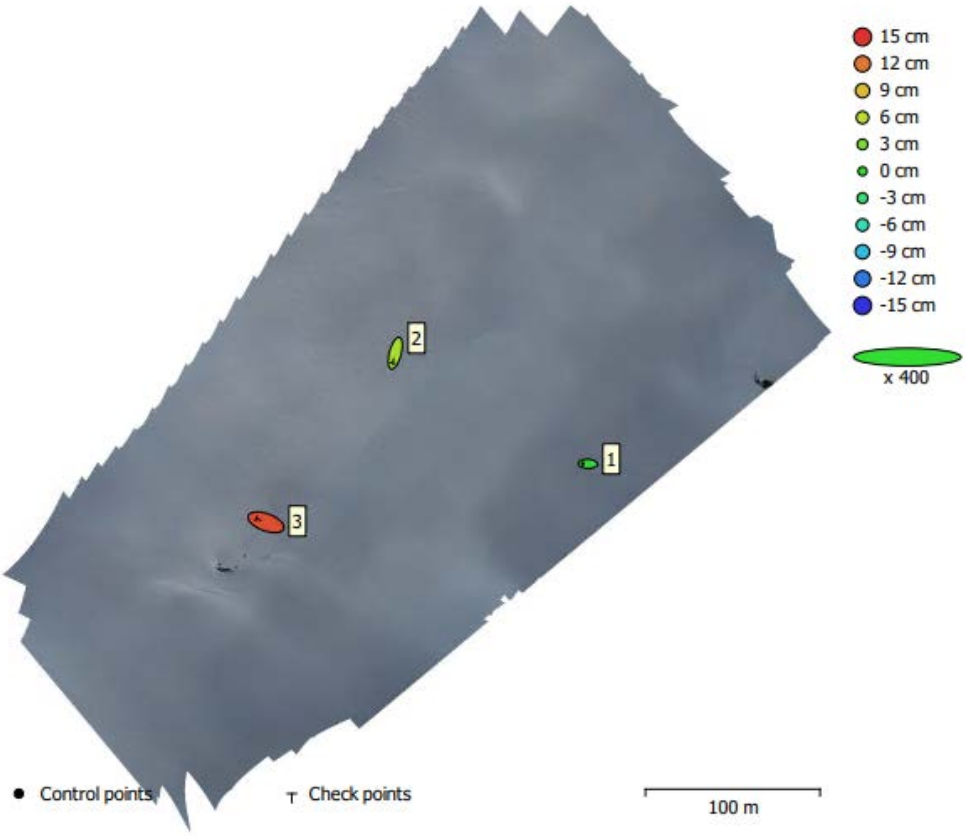

Figure 5-5. Photogrammetric reconstruction (orthomosaic depicted) over test area B with ground control point (GCP) locations marked; GCP 1 used for bundle adjustment control while remaining 2 GCP used as check points.

Table 5-4. Control and check point RMSE, using a single control point (see Figure 5-5).

Count	X error (cm)	Y error (cm)	Z error (cm)	XY error (cm)	Total (cm)
1 (Control)	1.46	0.0564	0.223	1.46	1.48
2 (Check)	2.03	2.17	10.4	2.97	10.8

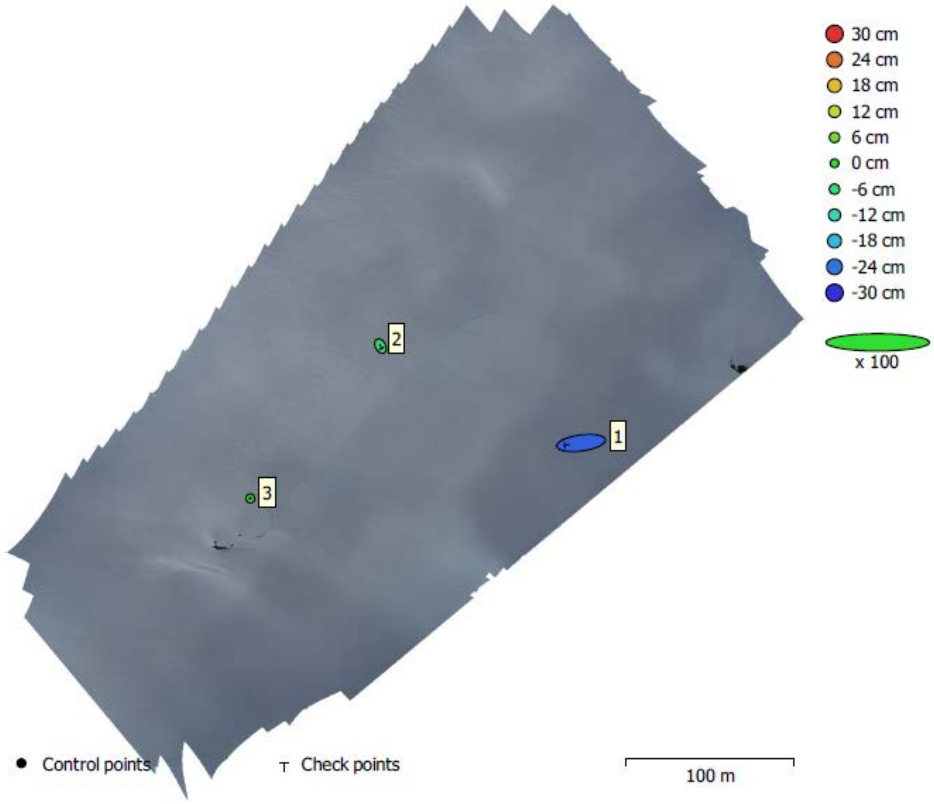

Figure 5-6. Photogrammetric reconstruction (orthomosaic depicted) over test area B with ground control point (GCP) locations marked; GCP 3 used for bundle adjustment control while remaining 2 GCP used as check points.

Table 5-5. Control and check point RMSE, using a single control point (see Figure 5-6).

Count	X error (cm)	Y error (cm)	Z error (cm)	XY error (cm)	Total (cm)
1 (Control)	0.104	0.236	0.179	0.258	0.314
2 (Check)	13.8	2.63	18.76	14.1	23.5

Effect of lighting conditions on image and model quality

Test area B was surveyed using a terrain-following, RTK-enabled mission on two subsequent days (30.3 and 31.3) under different lighting conditions. The lighting (solar illumination) during the UAS surveys had a significant effect on the resulting photogrammetric models. For the survey conducted on 30.3, 161 of the 375 total images could not be aligned in the initial bundle adjustment step, as presented in Figure 5-7. For the survey conducted on 31.3.22, all 375 images were successfully aligned, as depicted in Figure 5-8. The weather was cloud-free on both days, but sun angle and condition (age) of the snow surface may have had an effect on the image quality.

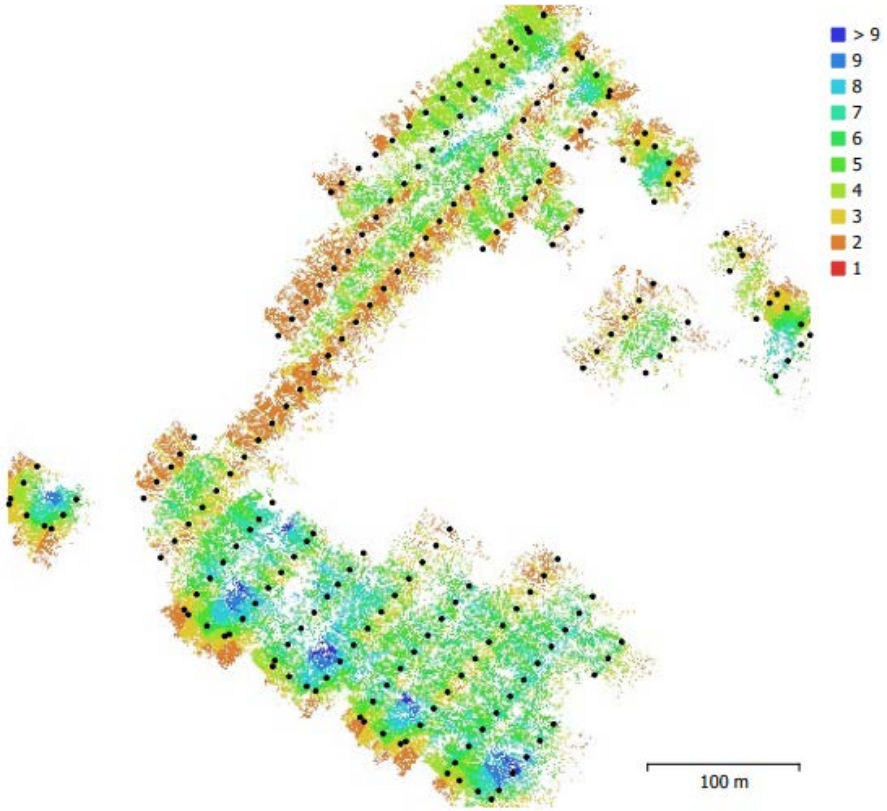

Figure 5-7. Photogrammetric reconstruction (sparse point cloud depicted) for data collected on 30.3.22 over test area B; colour scale indicates number of overlapping images.

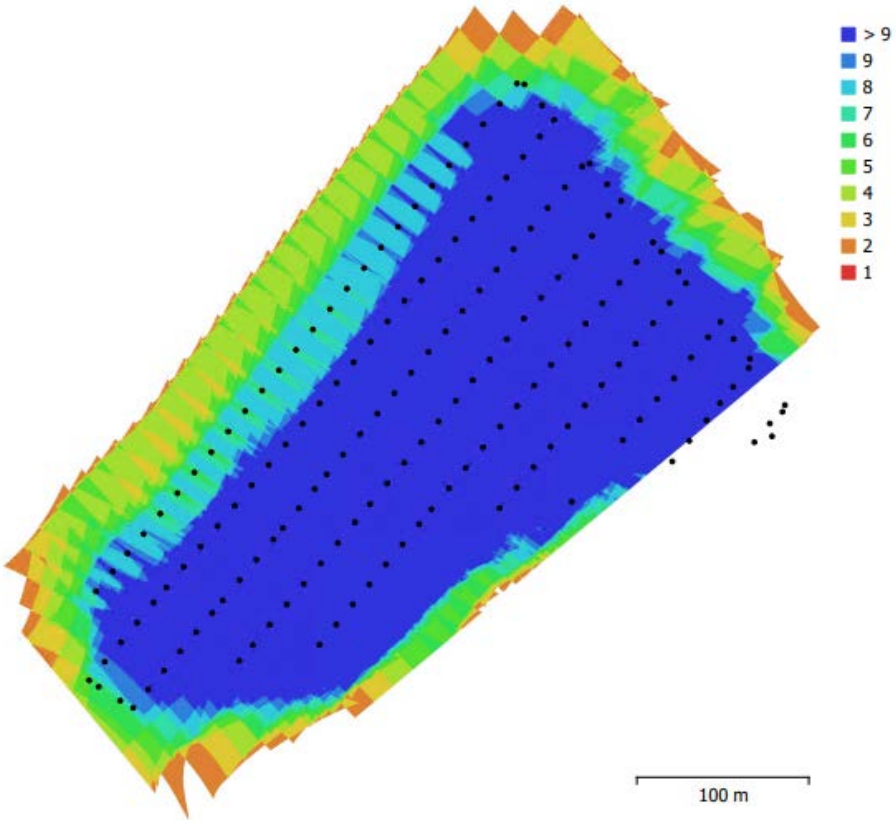

Figure 5-8. Photogrammetric reconstruction (image overlap map depicted) for data collected on 31.3 over test area B; colour scale indicates number of overlapping images.

Test area C was surveyed using a terrain-following, RTK-enabled mission. The absolute accuracy of the model could not be evaluated due to lack of ground control. Final products including digital surface models and ortho-mosaics for all three test areas are presented in Section 5.7.

5.4.2 Snowpack observations

Snowpack observations carried out by the GEOSFAIR team during the test week are described in section 1.3.

In addition to the observations described there, thermal imaging was conducted on the snow pit surfaces at site A2-1, using a Fluke Ti-400 series handheld camera, as illustrated in Figure 1-8. Surface temperatures were recorded for each pixel within the thermal images (two examples given in Figure 5-7). The so measured surface temperatures correlated well with temperatures measured using a conventional thermometer.

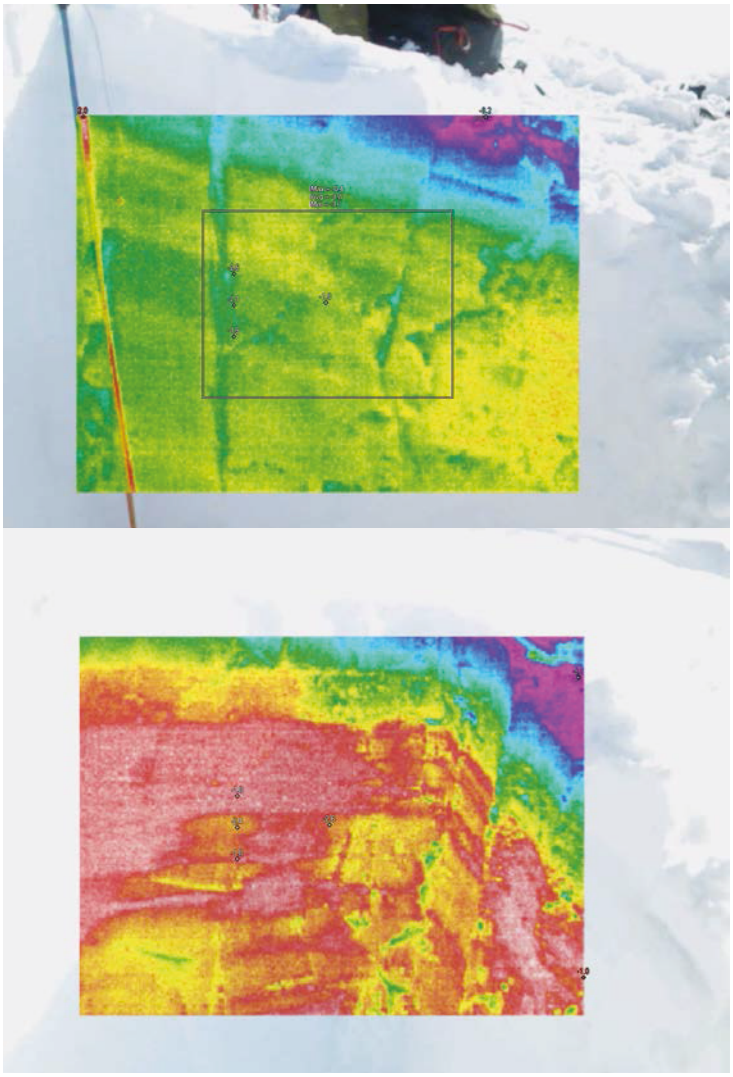

Figure 5-9. Examples of thermal camera images at site A2-1 captured with the handheld Fluke instrument; colour-scale is relative to maximum measured temperature range in each image subset.

5.5 Adjustments and lessons learned

Several equipment challenges were encountered in the field. Specifically, the DJI Phantom RTK aircraft and controller had some limitations. Described briefly in the points below are the challenges and some mitigating factors that were considered:

- It was often the case that an RTK fix using NTRIP virtual base station connection could not be achieved from the ground with a single-antenna UAS in the Grasdalen valley. It was however possible to take off manually in GNSS-only mode and acquire an RTK fix in the air before beginning a planned mission.
- At start and end of planned missions, maximum flight altitude must be considered carefully. A measure to avoid exceeding maximum allowable flight

altitude was to fly manually to the start and from finish of automated missions. Alternatively, additional waypoints can be added in the flight plan before and after mission execution.
- Camera exposure settings, especially default settings, may lead to poor data capture, particularly when acquiring photos in very bright conditions on snow, where shutter speed is very high and aperture size is reduced to a minimum. A possible measure to address poor image quality is to use manual camera settings and a greater altitude / slower flight speed to achieve acceptable exposure while minimizing motion blur.
- It was often difficult to maintain VLOS when using a small, white-coloured aircraft against a snow-covered background. The visibility of the aircraft could be improved by applying a contrasting colour to the aircraft body.

Additional equipment challenges were encountered with the FLIR Vue Pro R thermal camera payload. Described in the points below are the challenges and some mitigating factors that were considered:

- The camera gimbal was susceptible to faulty compensation and subsequently overheating, which also affected SD card detection and Bluetooth transmission.
- The payload mass and the balance point of the payload made it impractical to fly with a Phantom aircraft.
- Correct on-aircraft power supply for the gimbal and camera must be considered carefully.

5.6 Future Activities

Future work should focus on the following activities:

- Surveys performed in adverse lighting and/or weather conditions using different UAS camera sensors;
- Direct comparisons between photogrammetry and lidar scans to test sensitivity and relative accuracy;
- Airborne thermal imaging surveys validated with on-ground temperature measurements;
- Terrain-following mission planning without need for uploading individual digital elevation models;
- Third-party mission planning software using software developer kit (SDK) version of aircraft controller.

5.7 Preliminary products

Digital surface model and ortho-mosaic products generated for all three test areas are presented in Figure 5-10 through Figure 5-14.

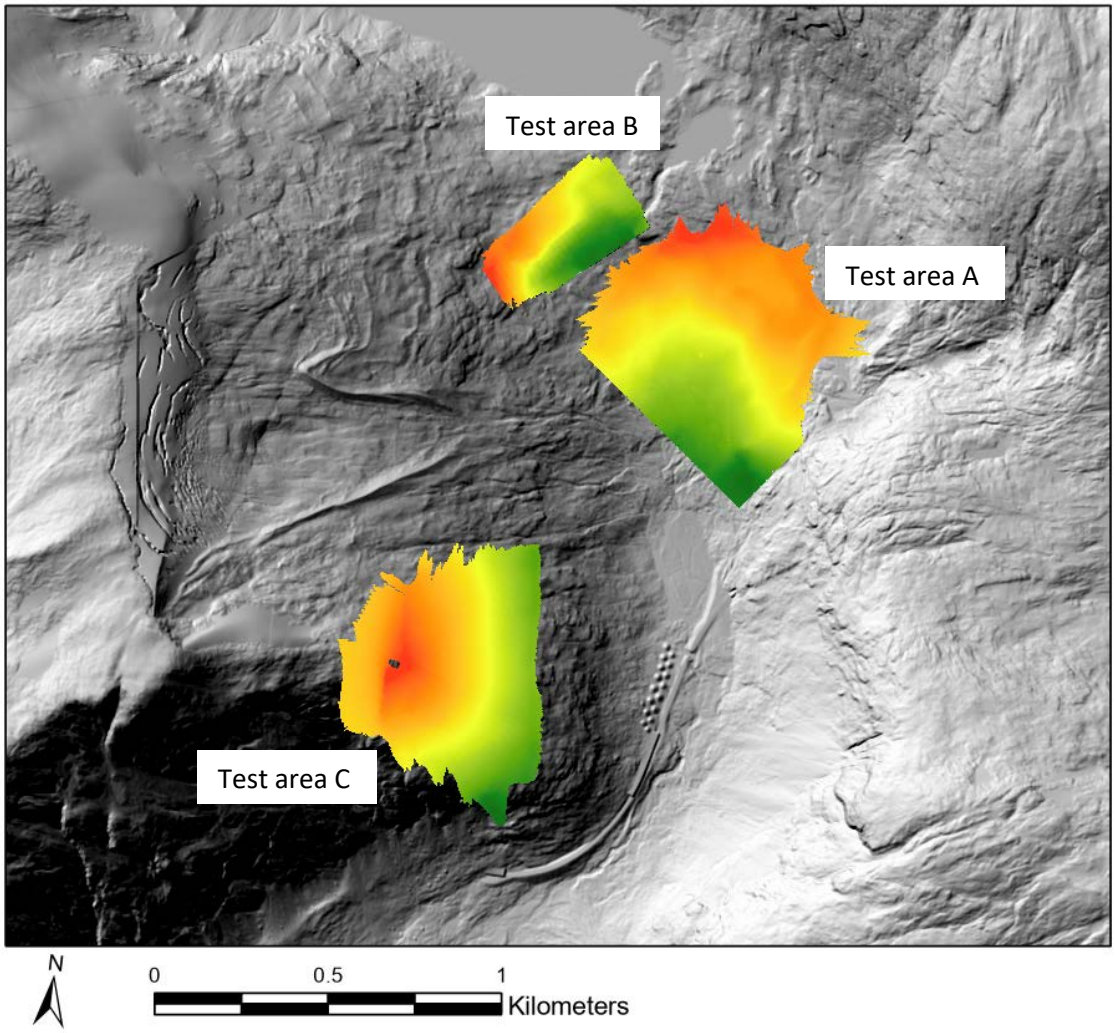

Figure 5-10. Digital surface models generated for all three test areas depicted atop a hillshade map; colour scale is relative to each individual test area and is shown for illustration purposes only.

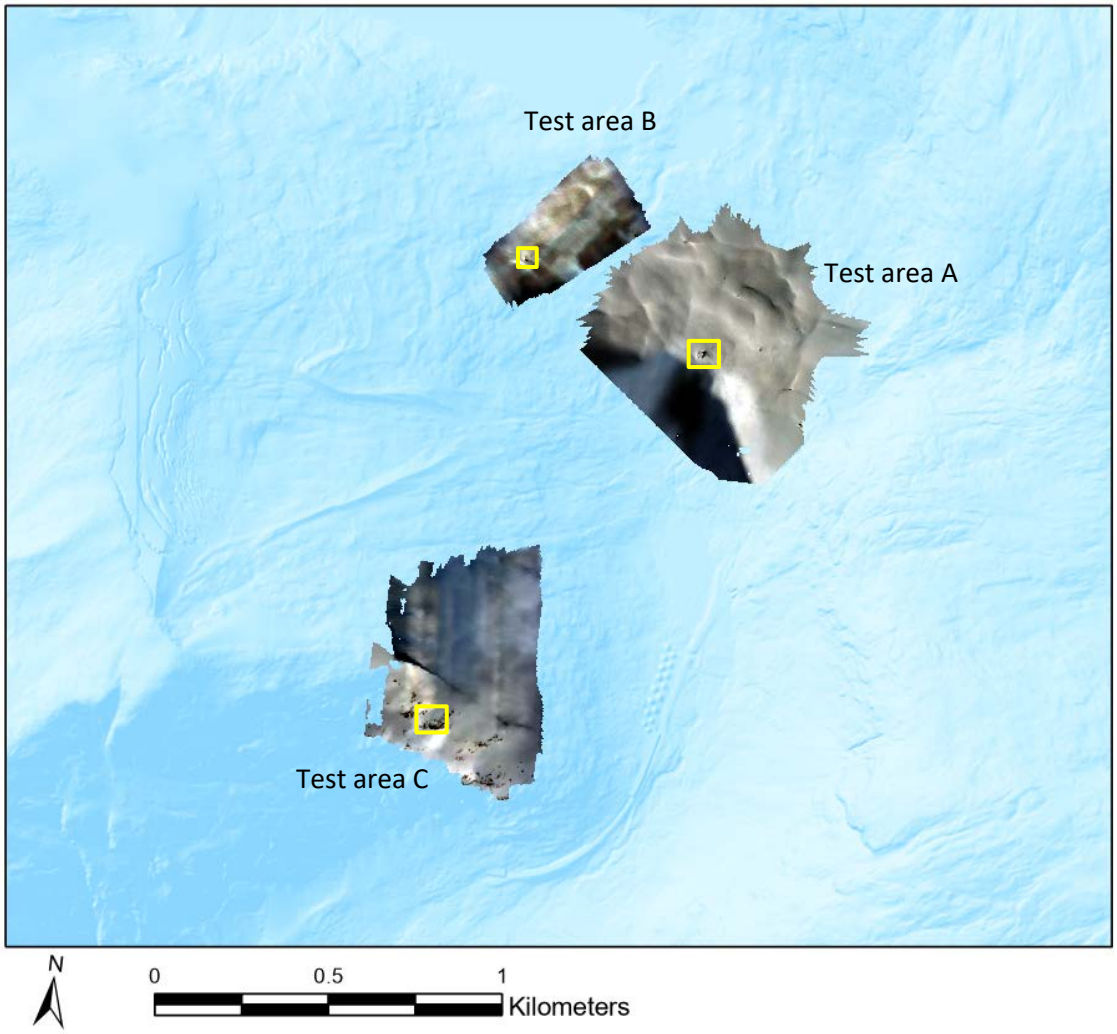

Figure 5-11. Ortho-mosaics generated for all three test areas depicted atop a hillshade map; close-up of area within the box in test area A survey is presented in Figure 5-12, while close-up within test areas B and C are presented in Figure 5-14 and Figure 5-16, respectively.

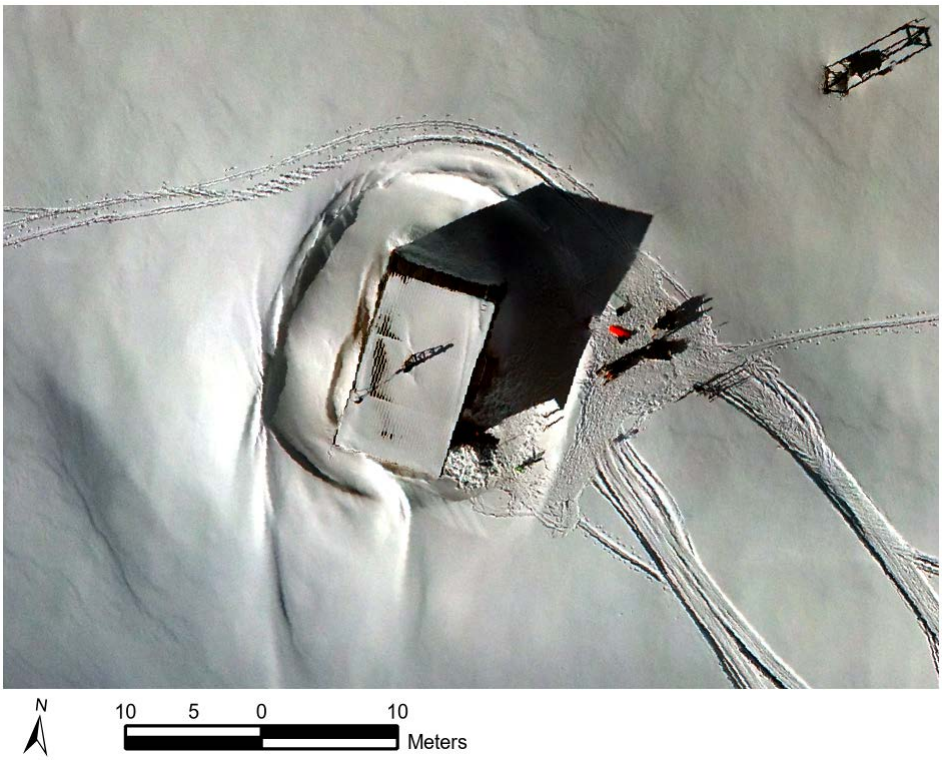

Figure 5-12. Close-up of area within the highlighted box in test area A in Figure 5-11 depicting Fonnbu station; average ground resolution of the survey was 3.5 cm/pixel.

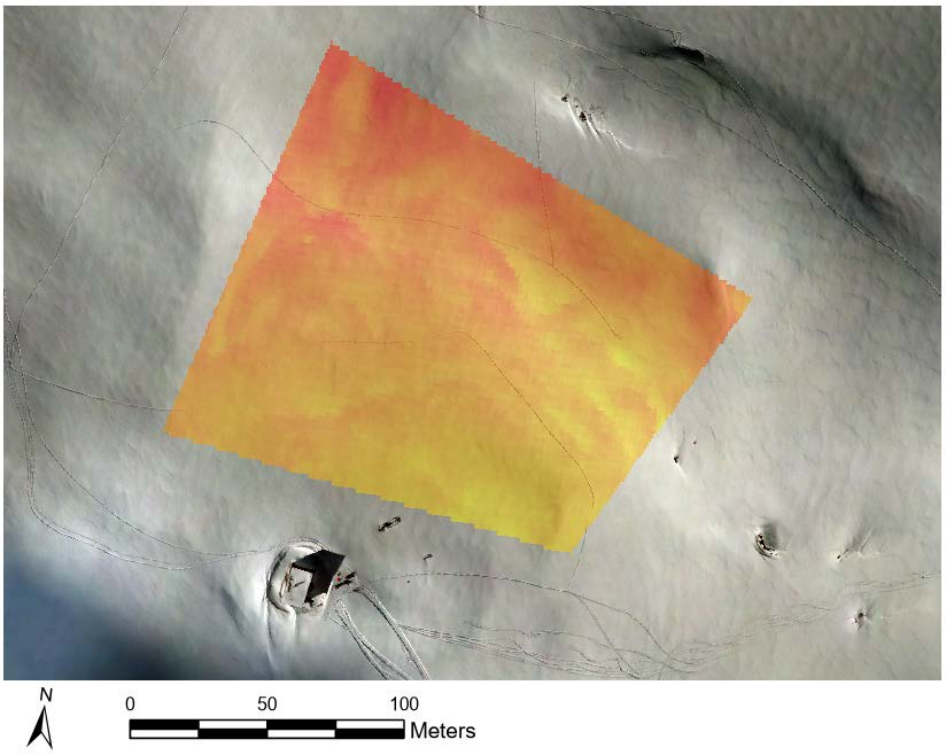

Figure 5-13. Snow height map for test area A based on terrain model by national mapping authority; colour scale is relative to test area with snow height increasing with warmth.

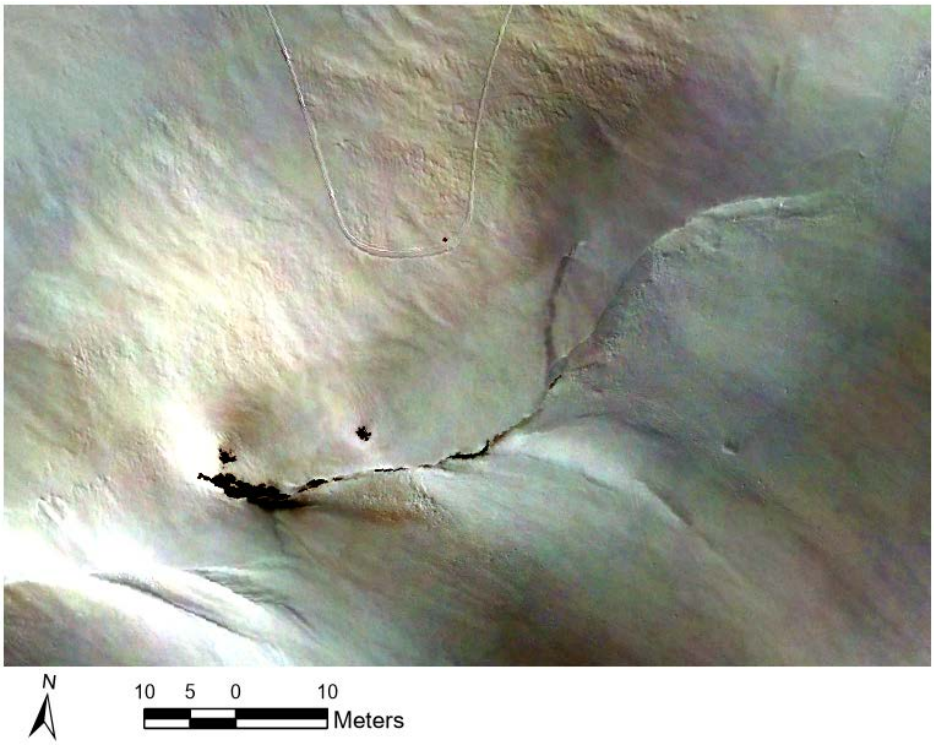

Figure 5-14. Close-up of area within the highlighted box in test area B in Figure 5-11; average ground resolution of the survey was 1.6 cm/pixel.

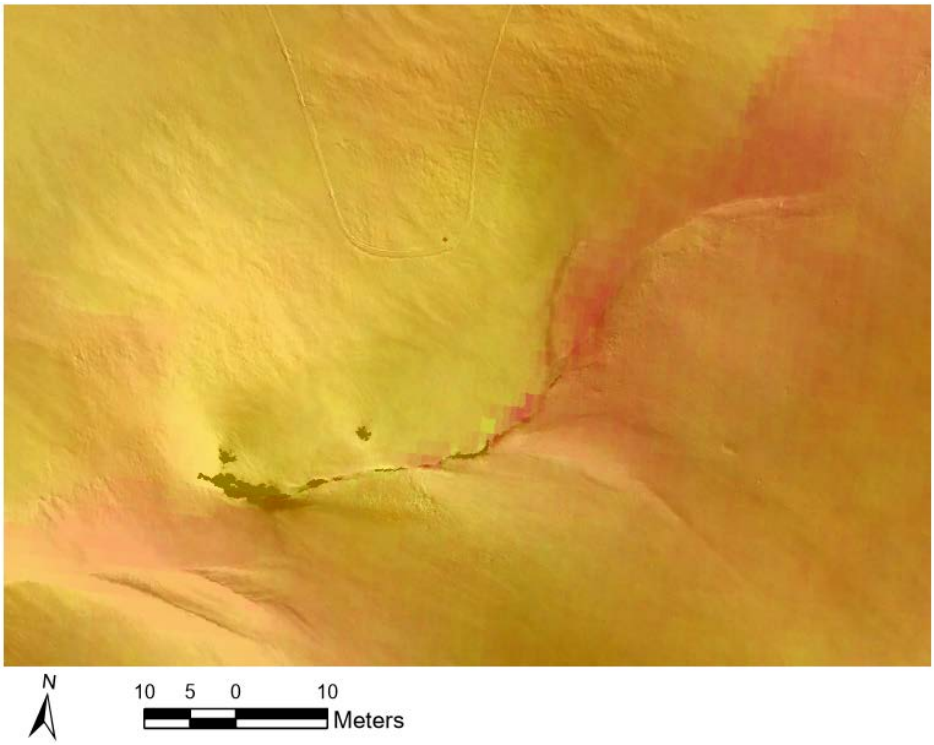

Figure 5-15. Snow height map in test area B based on terrain model by national mapping authority; colour scale is relative to test area with snow height increasing with warmth.

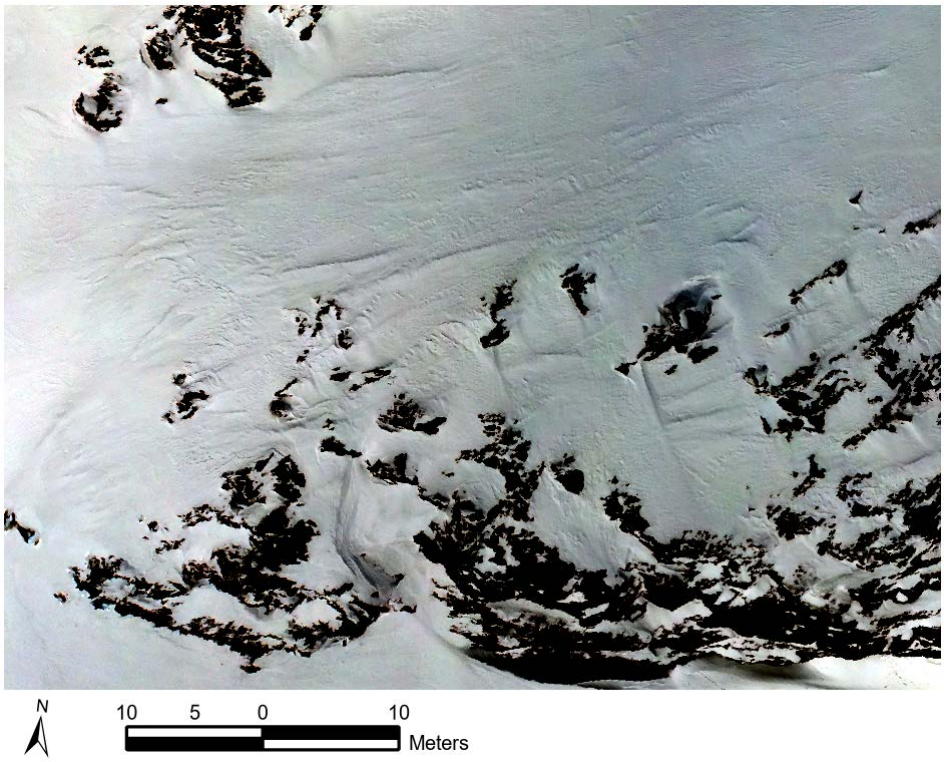

Figure 5-16. Close-up of area within the highlighted box in test area C in Figure 5-9; average ground resolution of the survey was 1.5 cm/pixel.

6 Discussion and Conclusions

This report documents a field test conducted as part of the GEOSFAIR (Geohazard Survey from Air) research project (Innovation Project for the Public Sector, Research Council of Norway grant no. 321035). The test was completed at NGI's Fonnbu avalanche research station. The project team included staff from the Norwegian Public Roads Administration (NPRA), the Norwegian Geotechnical Institute (NGI), and the research organization SINTEF (staff from both the Digital and the Industry groups).

The overall purpose was to test UAS-borne sensors and to collect data in field conditions that could be used to assess and monitor snow avalanche hazard. A series of flights and sensor measurements were carried out over four pre-defined test areas. The UAS-based measurements were complemented by snow pit characterization in three of the four test areas. The findings from this test will ultimately be used to develop tools in support of NPRA's processes for monitoring snow avalanches and supporting operational decisions related to avalanche risk.

In addition to testing snow measurement technologies, this test explored the operations of UAS flight planning, communications systems, flight controls, automated flights and the sensor and imaging technologies in realistic fields conditions. In most cases the UAS worked well, but the test also highlighted limitations that will need to be addressed before these tools can be used operationally. The technologies used during the test provided promising data about the snowpack and the terrain that will be helpful to NPRA staff as they monitor roadside avalanches. However, each technology also had challenges which will be addressed as GEOSFAIR continues.

Photogrammetry: In general, the photogrammetry results, obtained by applying Structure-from-Motion processing software to UAS-collected images, provided accurate information about snow heights and about the nature of the snow surface. The photogrammetry results had limitations due to digital noise and non-matched images caused by lack of recognisable surface features. In addition, GNSS positioning errors limited some results, and these errors were often related to the time required to acquire GNSS satellite signals and to achieve an accurate GNSS fix. High quality photogrammetry results also required that the UAS were flown over the area of interest using effective terrain-following flight paths with suitable image overlap and flight altitude.

Lidar: The results from the lidar sensors carried on UAS during the test provided accurate snow height and information about the terrain and the nature of the snow surfaces in the test areas. Elevation maps generated from the lidar data were compared to elevation maps derived using photogrammetry.

Ground Penetrating Radar: The field test findings suggested that GPR can provide quantitative measures concerning snow height, snow properties and layering. This information can be correlated with snow pits, photogrammetry, lidar and other forms of measurements. During the test, the GPR data collection, while mounted on a UAS, had

experienced electronic failure in cold weather (some of the GPR data for the test was successfully collected on a sled). The test results suggest that to collect suitable GPR data, additional work will be needed to determine the correct altitude and flight speed to allow the UAS's terrain-following algorithm to effectively use radar altimeter measurements.

Imaging Spectrometer: A spectral camera was tested to determine if this technology could infer grain size of the snow. Collecting this information over time during a winter season could be used to build a model of the layers in the snowpack. Both handheld and UAS images were collected, and the results were not optimal for discriminating snow types. The test did help develop a workflow for using multispectral images which require considerable post processing. Future work will develop a modular sensor package better for snow analysis and an analysis pipeline that will enable simpler data capture and support in-field validation and inspection of the data.

Thermal Camera: Images collected by a thermal camera (both handheld and UAS mounted) were tested to measure snow surface temperature. The measured surface temperatures correlated well with temperatures measured using a conventional thermometer. Future tests will explore the value of thermal images for avalanche monitoring.

Operations of the equipment: The test demonstrated the importance of operationally proofing and testing the equipment. The team had a number of equipment failures and, in many cases, long setup times before the cameras and sensors could be flown on the UAS. This is to be expected, particularly as this is the first field test in the GEOSFAIR project. Nonetheless, this also indicates that if this technology is to be used on a routine basis by NPRA staff, the equipment needs to be well tested, and the staff will need to be familiar and trained in operation of the UAS and sensors.

Linking UAS collected data to field conditions. The information from the sensors will continue to need to be linked to actual field conditions to confirm that the results are usable by avalanche experts. In this test, the sensors did provide data but the value of this data for the NPRA's operations will require continued validation. This challenge is exacerbated by the difficulty of manually quantifying snowpack conditions. Future collection of detailed snow surface data for calibration should be based on established, instrument-based methods for snow grain classification. This validation will occur as the team continues the GEOSFAIR project.

Locational tools: Global navigation satellite systems were critical for operating the UAS, for registering many of the data collection efforts, and for simply locating the resulting snow data findings. The team, at times, had challenges related to acquiring precise positioning using satellites and the RTK ground stations.

Data processing. The processing of the sensor data was completed by each work package team with expertise in their technology. This worked well but does indicate that each sensor, as ultimately used by the NPRA, will probably require separate training and different types of expertise. For example, processing and analysing GPR image data will

require different software and a different skill set from processing optical images. Initial processing of survey data should ideally be done shortly after flight, to check data quality and to allow adjustments along the way. This will require a pool of NPRA staff familiar with the data and processing software.

Control points: Ground control points for registering the location of survey points in images collected by the UAS was important and will need to be accommodated in future tests and during routine operations by the NPRA. For many of the sensor technologies, terrain-following tools and software for operating the UAS at suitable data collection altitudes caused challenges during this test and will require further investigation.

Weather conditions: Overall, the weather conditions were good for the Fonnbu test. It is uncertain, at this point, what type of data could be collected in weather that was windy, cold, or had active precipitation. Tied to weather conditions was the difficulty of maintaining visual line of sight (VLOS) when using small, or light-coloured aircraft against a snow-covered background. Tracking an aircraft could be an even greater challenge in bad weather. The visibility of the aircraft could be improved by applying a contrasting colour to the aircraft body.

Future Steps

The findings from this test will inform and guide the next series of GEOSFAIR field tests and activities. They will include:

- Continue testing of UAS with different sensors including RGB camera for photogrammetry, lidar scanner, GPR, thermal camera, and multispectral camera.
- More testing in adverse lighting and/or weather conditions using different UAS sensors and cameras.
- Investigate different sources of GNSS positioning errors and what is required for ground control points.
- Explore different operational parameters and software (such as terrain-following, flight path-overlap, etc) for the UAS to support quality data collection for different devices.
- Explore streamlining workflows and create checklists to ensure quality data including testing different opportunities for automated/semi-automated data flow, from sensor data to results presented in a web viewer.
- Explore how to parameterize the snow types efficiently to use for making models. This will support linking manual observation with sensor collected data.
- Explore different approaches to onsite or remote data collection, whether the drone is operated by the avalanche expert, a contractor in the field (with the avalanche expert in back-office) or even an autonomous drone station.

Appendix A

MAP OF TEST AREA

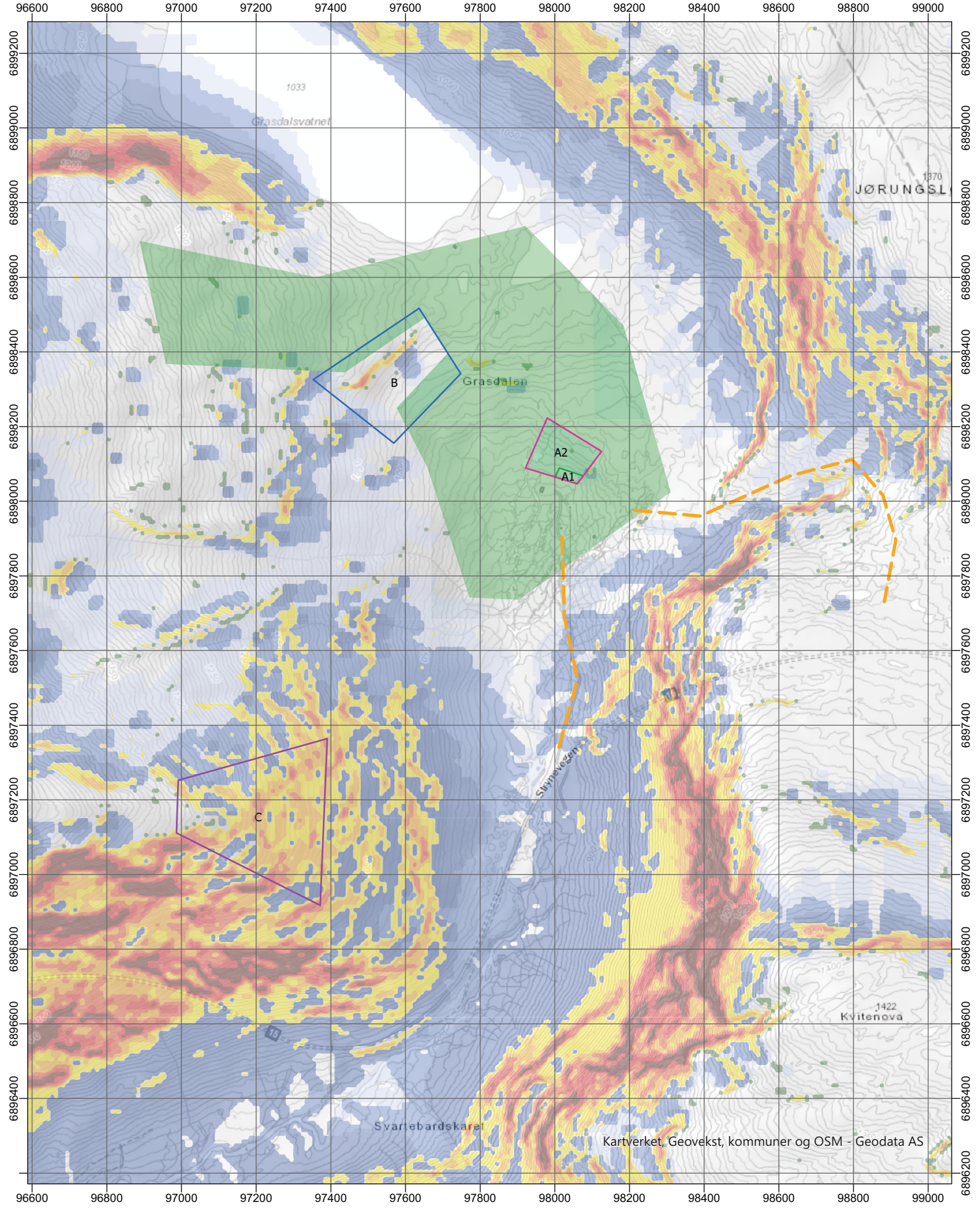

Operation area
Critical route
A1
A2
B
C

27-30
30-35
35-40
40-45
45-50
50-90

Utløp α = 32
Utløp α = 27
Utløp α = 23 (95%)

0 250 500 m

N

Critical route: Specific SJA and avalanche assessment required
Operation area: Avalanche assessment not required

Appendix B

METEOROLOGICAL DATA

Contents

B1 Key weather parameters, Fonnbu station, March 20, 2022 and April 2, 2022

B1.1 Hourly precipitation

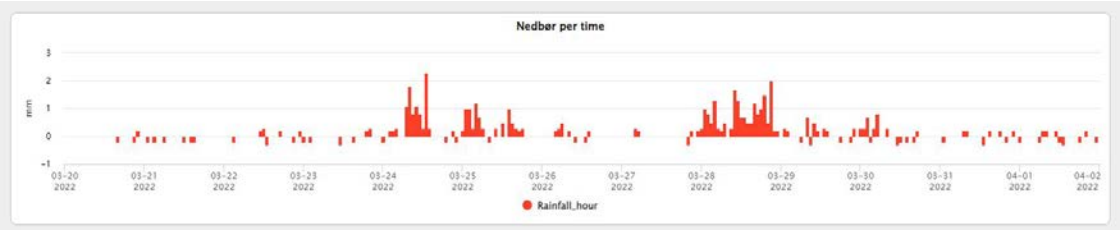

B1.2 Snow height

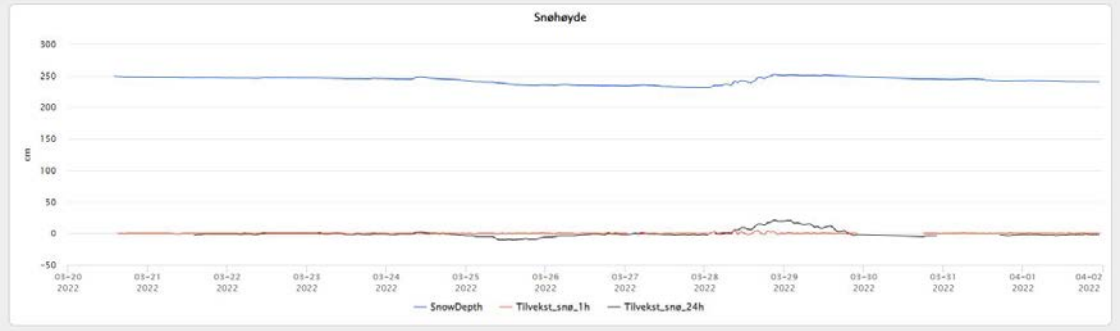

B1.3 Radiation, albedo

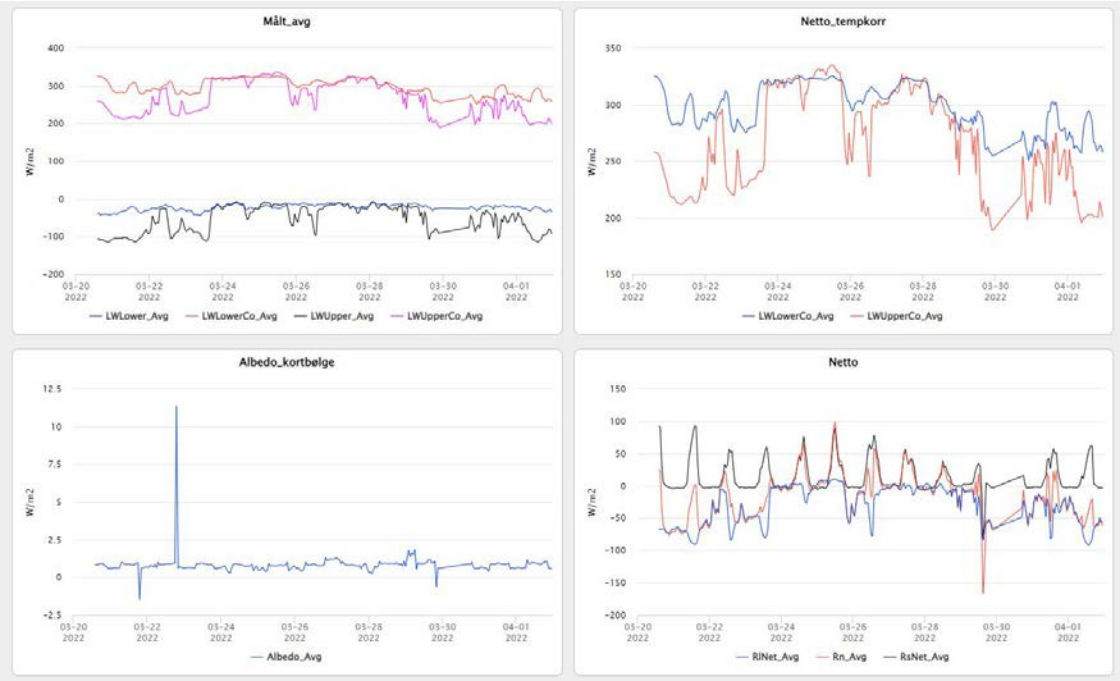

B1.4 Temperature

B1.5 Wind speed and wind direction

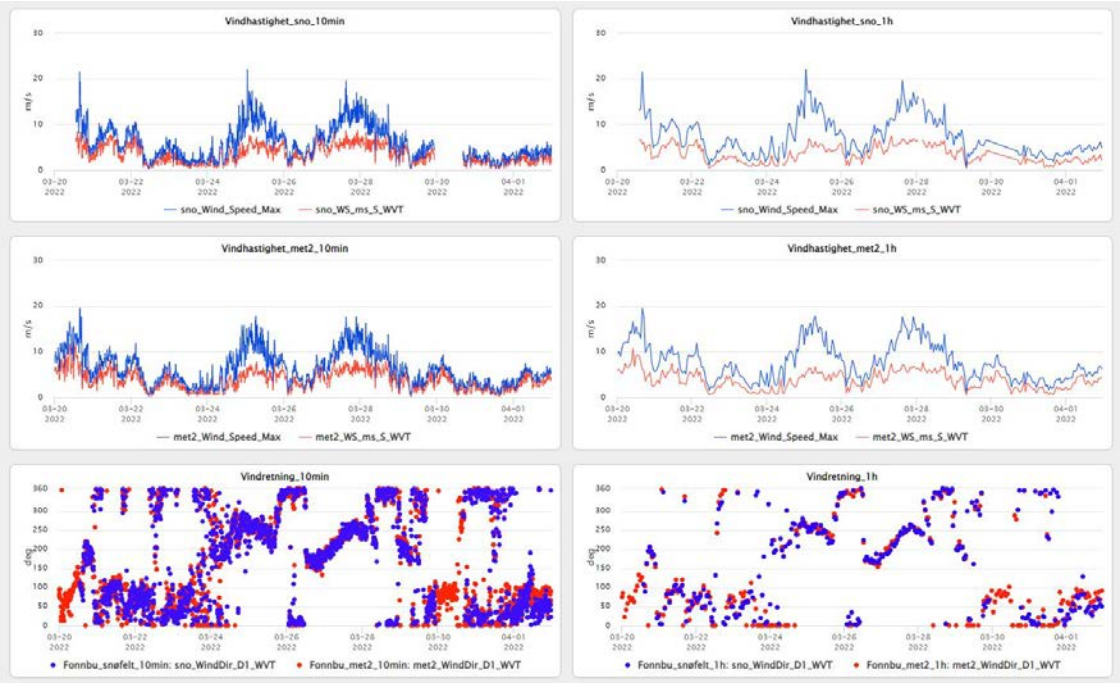

Kontroll- og referanseside/ Review and reference page

Dokumentinformasjon/*Document information*		
Dokumenttittel/*Document title* Field test activity report - Fonnbu March 2022		**Dokumentnr./*Document no.*** 20210309-01-R
Dokumenttype/*Type of document* Rapport / Report	**Oppdragsgiver/*Client*** The Research Council of Norway	**Dato/*Date*** 2022-11-08
Rettigheter til dokumentet iht kontrakt/ *Proprietary rights to the document according to contract* Oppdragsgiver / Client		**Rev.nr.&dato/*Rev.no.&date*** 0 / 2022-11-08
Distribusjon/*Distribution* ÅPEN: Skal tilgjengeliggjøres i åpent arkiv (BRAGE) / OPEN: To be published in open archives (BRAGE)		
Emneord/*Keywords* GEOSFAIR, NPRA, NGI, SINTEF, UAS, AVALANCHE, SNOW		

Stedfesting/*Geographical information*	
Land, fylke/*Country* Norway	**Havområde/*Offshore area***
Kommune/*Municipality*	**Feltnavn/*Field name***
Sted/*Location*	**Sted/*Location***
Kartblad/*Map*	**Felt, blokknr./*Field, Block No.***
UTM-koordinater/*UTM-coordinates* **Zone: East: North:**	**Koordinater/*Coordinates*** **Projection, datum: East: North:**

Dokumentkontroll/*Document control*

Kvalitetssikring i henhold til/*Quality assurance according to NS-EN ISO9001*

Rev/ *Rev.*	**Revisjonsgrunnlag/*Reason for revision***	**Egenkontroll av/ *Self review by:***	**Sidemanns-kontroll av/ *Colleague review by:***	**Uavhengig kontroll av/ *Independent review by*:**	**Tverrfaglig kontroll av/ *Interdisciplinary review by:***
0	Original document	2022-08-19 Regula Frauenfelder	2022-11-02 Sean Salazar		

Dokument godkjent for utsendelse/ *Document approved for release*	**Dato/*Date***	**Prosjektleder/*Project Manager***
	8 November 2022	Tore Kvalstad

Norwegian Public Roads Administration

NGI (Norwegian Geotechnical Institute) is a leading international centre for research and consulting within the geosciences. NGI develops optimum solutions for society and offers expertise on the behaviour of soil, rock and snow and their interaction with the natural and built environment.

NGI works within the following sectors: Geotechnics and Environment – Offshore energy – Natural Hazards – GeoData and Technology

NGI is a private foundation with office and laboratories in Oslo, a branch office in Trondheim and daughter companies in Houston, Texas, USA and in Perth, Western Australia

www.ngi.no

NGI (Norges Geotekniske Institutt) er et internasjonalt ledende senter for forskning og rådgivning innen ingeniørrelaterte geofag. Vi tilbyr ekspertise om jord, berg og snø og deres påvirkning på miljøet, konstruksjoner og anlegg, og hvordan jord og berg kan benyttes som byggegrunn og byggemateriale.

Vi arbeider i følgende markeder: GeoMiljø – Offshore energi – Naturfare – GeoData og teknologi.

NGI er en privat næringsdrivende stiftelse med kontor og laboratorier i Oslo, avdelingskontor i Trondheim og datterselskaper i Houston, Texas, USA og i Perth, Western Australia.

www.ngi.no

OSLO
TRONDHEIM
HOUSTON
PERTH

NORWEGIAN GEOTECHNICAL INSTITUTE
NGI.NO

Main office
PO Box 3930 Ullevaal St.
NO-0806 Oslo
Norway

Trondheim office
PO Box 5687 Torgarden
NO-7485 Trondheim
Norway

T (+47)22 02 30 00
NGI@ngi.no

BIC NO. DNBANOKK
IBAN NO26 5096 0501 281
ORGANISATION NO.
958 254 318MVA

ISO 9001/14001
CERTIFIED BY BSI
FS 32989/EMS 612006

Statens vegvesen
Pb. 1010 Nordre Ål
2605 Lillehammer

Tlf: (+47) 22 07 30 00

firmapost@vegvesen.no

ISSN: 1893-1162

vegvesen.no

Tryggere, enklere og grønnere reisehverdag